Indolylarylsulfones carrying a Heterocyclic Tail as Very Potent and Broad Spectrum HIV-1 Non-Nucleoside Reverse Transcriptase Inhibitors

Valeria Famiglini,[†] Giuseppe La Regina,[†,*] Antonio Coluccia,[†] Sveva Pelliccia,[≠] Andrea Brancale,[‡] Giovanni Maga,[§] Emmanuele Crespan,[§] Roger Badia,[∞] Eva Riveira-Muñoz,[∞] José A. Esté,[∞] Rosella Ferretti,[°] Roberto Cirilli,[°] Claudio Zamperini,[ø] Maurizio Botta,[ø] Dominique Schols,[fl] Vittorio Limongelli,[≠] Bruno Agostino,[≠] Ettore Novellino,[≠] and Romano Silvestri[†]

[†]Istituto Pasteur - Fondazione Cenci Bolognetti, Dipartimento di Chimica e Tecnologie del Farmaco, Sapienza Università di Roma, Piazzale Aldo Moro 5, I-00185 Roma, Italy

[≠]Dipartimento di Farmacia, Università di Napoli Federico II, Via Domenico Montesano 49, I-80131, Napoli, Italy

[‡]Welsh School of Pharmacy, Cardiff University, King Edward VII Avenue, Cardiff, CF10 3NB, UK

[§]Institute of Molecular Genetics IGM-CNR, National Research Council, via Abbiategrasso 207, I-27100 Pavia, Italy

[∞]AIDS Research Institute - IrsiCaixa, Hospitals Germans Trias i Pujol, Universitat Autonóma de Barcelona, 08916 Badalona, Spain

[°]Dipartimento del Farmaco, Istituto Superiore di Sanità, Viale Regina Elena 299, I-00161 Roma, Italy

[ø]Dipartimento di Biotecnologia Chimica e Farmacia, Università di Siena, Via Aldo Moro 2, I-53100 Siena, Italy

[fl]Department of Microbiology and Immunology, University of Leuven, Minderbroedersstraat 10, 3000 Leuven, Belgium

ABSTRACT

We synthesized new indolylarylsulfone (IAS) derivatives carrying a heterocyclic tail at the indole-2-carboxamide nitrogen as potential anti-HIV/AIDS agents. Several new IASs yielded EC_{50} values <1.0 nM against the HIV-1 WT and mutant strains in MT-4 cells. The enantiomer *(R)*-**11** proved to be exceptionally potent against the whole viral panel; in the RT screening assay it was remarkably superior to NVP and EFV and comparable to ETV. The binding poses were consistent with the one previously described for the IAS NNRTIs. Docking studies showed that the methyl group of the *(R)*-**11** pointed towards the cleft created by the K103N mutation, differently from the corresponding group of *(S)*-**11**. By calculating the solvent accessible surface, we observed that the exposed area of the RT in complex with *(S)*-**11** was larger than the area of the *(R)*-**11** complex. Compounds **6** and **16** and the enantiomer *(R)*-**11** represent novel robust lead compounds of the IAS class.

INTRODUCTION

Human immunodeficiency virus type 1 (HIV-1) infection and acquired immunodeficiency syndrome (AIDS) are clinically treated with antiretroviral agents,[1] as the development of an effective HIV-1 vaccine still remains problematic.[2] Antiretroviral drugs used in the treatment of HIV infection may be viewed as falling into nucleoside reverse transcriptase inhibitors (NRTIs) that also include the nucleotide agents, no nucleoside reverse transcriptase inhibitors (NNRTIs), protease inhibitors (PIs), fusion inhibitors (FIs), entry inhibitors - CCR5 co-receptor antagonists, and HIV integrase strand transfer inhibitors (INSTIs). Such antiretroviral agents are administered singly or combined into multi-drug combination products.[3,4]

The clinical treatment for HIV/AIDS takes advantage of the multiple benefits of the antiretroviral therapy (ART), also known as active antiretroviral therapy (HAART). ART abides of two or at least three antiretroviral drugs from different drug classes. The life-saving ART regimens suppress the HIV-1 replication and slow down the progression of viral infection, particularly in early stages of the disease, maintaining plasma viremia below the detection level in most patients undergoing treatment for at least six months.[5]

Nevirapine (NVP), Delavirdine (DLV) and Efavirenz (EFV) are first-generation NNRTIs; it is recognized that such agents rapidly develop drug resistance; in particular the K103N and Y181C mutations are prevalent from clinical HIV-1 isolates.[6] Newer NNRTIs, Etravirine (ETV) and Rilpivirine (RPV) were approved for use in drug combination to manage treatment-experienced HIV-1 infected people, and naïve and adult patients, respectively.[7] However, despite a significant progress, drug resistance and adverse effects continue to emerge in ART receiving patients.[8] These data underlines the need of new antiretroviral agents with improved and tolerability resistance profiles.

Chart 1. Structure of New IASs 4-20 and Reference Compounds 1-3.[a]

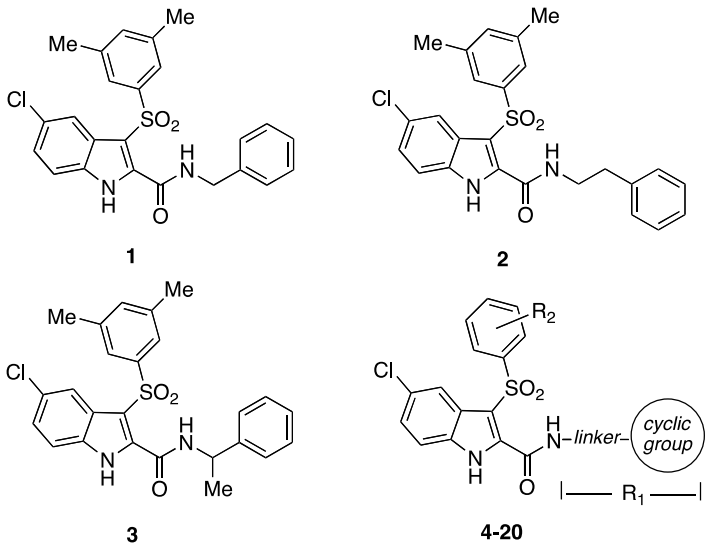

[a]**4-20**: R_1 = H; *cyclic group* = phenyl, pyridinyl, pyrimidinyl, heterocyclyl; *linker* = 0, CH_2, CH_2CH_2, CHMe, NH, NMe; R_2 = 3,5-Me_2, 2,6-Me_2, 2,6-Cl_2 (see Table 1).

In the indolylarylsulfone (IAS) HIV-1 NNRTI class, the two methyl groups at positions 3' and 5' of the 3-phenylsulfonyl moiety proved to ensure a broad spectrum of activity against mutant HIV-1 strains. The indole-2-carboxamide demonstrated to tolerate a wide diversity of substituents (natural or unnatural amino acids, hydroxyethyl moiety, Mannich bases) to provide IAS analogues with remarkable antiviral potency.[9]

The introduction of an additional aromatic nucleus to the parent compound resulted in NNRTIs with broad spectrum of activity against the mutant HIV-1 strains.[10] Accordingly, IAS derivatives bearing an additional (third) cyclic moiety linked through 1C or 2C spacer group the 2-carboxamide nitrogen (**1-3**) showed potent antiretroviral activity.[11,12] Therefore, we planned the synthesis of new inhibitors that would address this drug design strategy. The new IAS derivatives **4-20** showed potent HIV-1 inhibitory activity in the low nanomolar range (Chart 1 and Table 1).

Scheme 1. Synthesis of Carboxamides 4-20.[a]

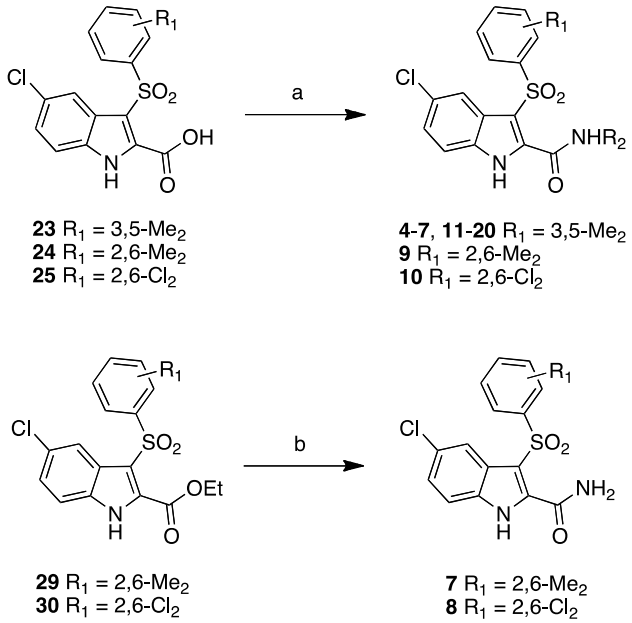

23 R_1 = 3,5-Me_2
24 R_1 = 2,6-Me_2
25 R_1 = 2,6-Cl_2

4-7, **11-20** R_1 = 3,5-Me_2
9 R_1 = 2,6-Me_2
10 R_1 = 2,6-Cl_2

29 R_1 = 2,6-Me_2
30 R_1 = 2,6-Cl_2

7 R_1 = 2,6-Me_2
8 R_1 = 2,6-Cl_2

[a]Reagents and reaction conditions: (a) amine, BOP reagent, triethylamine, anhydrous DMF, 25 °C, 12 h, yield (%) 40-82; (b) 30% NH_4OH, EtOH, 60 °C, overnight, yield (%) 32-35.

CHEMISTRY

Carboxamides **4**-**6** and **9**-**20** were synthesized by coupling reaction of the indole acids **21**,[9a] **22** and **23** with the appropriate amine in the presence of (benzotriazol-1-yloxy)tris(dimethylamino)-phosphonium hexafluorophosphate (BOP reagent) and triethylamine in anhydrous DMF at 25 °C for 12 h. On the other hand, esters **29** and **30** were transformed into the corresponding carboxamides **7** and **8** by heating at 60 °C with 30% ammonium hydroxide in ethanol (Scheme 1).

Scheme 2. Synthesis of Intermediates 22 and 23.[a]

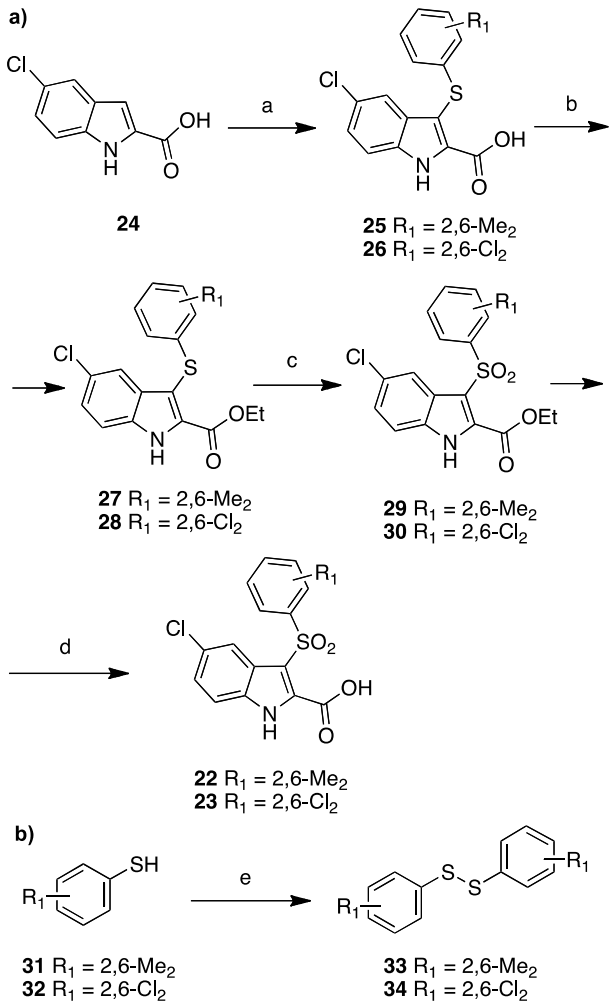

[a]Reagents and reaction conditions: a) (a) (i) NaH, anhydrous DMF, 25 °C, 10 min; (ii) DADS 110 °C, 12 h, (b) thionyl chloride, anhydrous EtOH, reflux, 12 h, yield (%) 51-62; (c) MCPBA, $CHCl_3$, 25 °C, 2 h, yield (%) 67-75; (d) LiOH, THF/H_2O, 25 °C, 48 h, yield (%) 85-96; b) (e) 1,3-dibromo-5,5-dimethylhydantoin, $CHCl_3$, 25 °C, 5 min, yield (%) 91-99.

The starting acids **22** and **23** were obtained by reaction of the proper diaryldisulfides (DADS) **33** or **34** with ethyl 5-chloro-1*H*-indole-2-carboxylic acid (**24**) in the presence of sodium hydride according to the Atkinson reaction[13] to provide the corresponding 3-arylthio-1*H*-indole-2-carboxylic acids **25** or **26**. Esterification was achieved by treating of **25**, **26** with thionyl chloride in anhydrous ethanol at 80 °C overnight to furnish the intermediates **27** or **28** (Scheme 2, panel a).

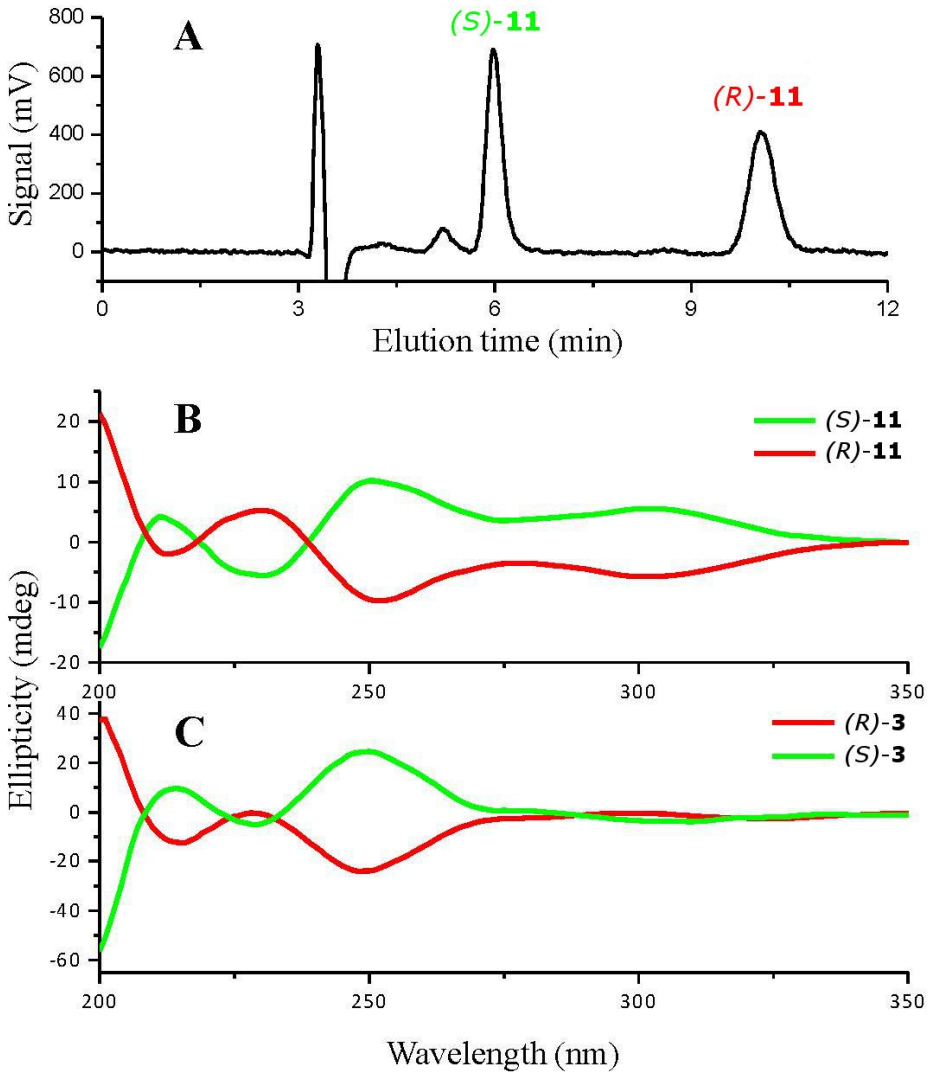

Figure 1. HPLC enantioseparation of **11** (panel A). Column Chiralcel OD 250 mm × 4.6 mm I.D.; detection, UV at 280 nm; mobile phase, *n*-hexane-ethanol 1:1 (v/v); flow rate, 1.0 mL min^{-1}; column temp. 25 °C. Comparison of the CD spectra of the enantiomers *(S)*-**11** and *(R)*-**11** (panel B) with those of (*R*)-**3** and (*S*)-**3** (panel C) recorded in ethanol at 20 °C.

Oxidation of **27** and **28** to the corresponding sulfones **29** and **30** was performed with 3-chloroperoxybenzoic acid (MCPBA) in chloroform at room temperature. Lithium hydroxide hydrolysis of the esters **29** and **30** afforded the required acids **22** and **23**, respectively. The DADSs **33** and **34** were prepared by oxidation of proper thiophenols in the presence of 1,3-dibromo-5,5-dimethylhydantoin (Scheme 2, panel b).

Direct enantioseparation of the racemic mixture (*R,S*)-**11** was performed by enantioselective HPLC using the cellulose derived Chiralcel OD chiral stationary phase (CSP) and the binary mixture *n*-hexane-ethanol 50:50 as a mobile phase (Figure 1A). The optimized analytical enantioselective method was scaled-up to a semi-preparative level to obtain mg-amounts of the pure enantiomers for the screening. The stereochemical characterization of *(S)*-**11** and *(R)*-**11** was performed by circular dichroism (CD) correlation method using the (*R*)-**3** and (*S*)-**3** pure enantiomers as reference samples (Figure 1B and 1C). The (*R*) configuration was empirically assigned to the more retained enantiomer *(S)*-**11** on the Chiralcel OD CSP, and the (*S*) configuration to the less retained enantiomer *(R)*-**11**.

RESULTS AND DISCUSSION

Independently on the substituent at the nitrogen atom at the position 2 of the indole, a large proportion of the new IASs inhibited the HIV-1 NL4-3 strain by fifty-percent (EC_{50} values) in the sub-nanomolar range of concentrations (MTT method). Compounds **4**, **5**, **6**, **8**, **12**, **13**, **17, 18** and **20**, were highly inhibitory to the HIV-1 replication at the lowest detectable nM concentration (Table 1). The majority of the new IASs were superior to the reference drugs NVP, EFV, and AZT. Unless **8**, the new IAS derivatives showed cytotoxic concentrations (EC_{50} values) >20000 nM. With the exception of **7**, **9** and **14**, the new derivatives showed selectivity indexes (SI = CC_{50}/EC_{50} ratio) >20000. Derivative **16**, showed the highest SI value (SI >282218) within the series; it was superior to NVP, EVF and AZT and comparable the reference IASs **1-3**. As expected for NNRTI,[14] compounds did not show inhibitory activity for HIV-2.

We initially synthesized the 4-pyridinyl derivative **4** by expelling the methylene spacer group. Compound **4** proved to be a potent inhibitor of the HIV-1 NL4-3 WT and K103N mutant strains (EC_{50} = 0.23 nM), but it was weakly effective against the K103N-Y181C double mutant strain (Table 2). Extrusion of the nitrogen atom from the pyridinyl ring of **4** resulted in an equipotent inhibitor of the

NL4-3 strain; compound **5** showed an interesting inhibition of the K103N-Y181C double mutant strain at EC_{50} = 2137 nM. Furthermore, we introduced two nitrogen atoms at the positions 2 and 4 of the benzyl group of **1** to obtain **6**. This new IAS derivative potently inhibited the NL4-3 WT strain (EC_{50} = 0.22 nM), K103N, Y181C and Y188L mutant strains (EC_{50} (nM) = 0.22, 0.22, 2.20 and 20.6, respectively). Most importantly, **6** proved to inhibit the K103N-Y181C double mutant strain with EC_{50} = 132 nM, being >28- and >2.5-fold more potent than NVP and EFV, respectively, and 16-fold superior to IAS **1**. Shifting the substituents of the 3-phenylsulfonyl moiety from 3',5' to 2',6' positions retained the antiretroviral activity only in the case of the 2',6'-dichloro derivatives **8** and **10** (compare with **7** and **9**).

The replacement of the phenyl group of **3** with a pyridinyl ring to obtain **11** resulted in a general improvement of the antiviral activity. Racemate **11** were found to be 3-fold more potent than **3** as inhibitor of the NL4-3 WT strain (EC_{50} = 0.2 nM). Against the Y181C, L100I and K103N-Y181C mutant strains IAS **11** was respectively 8- and 6- and 3-times superior to **3**. Such results prompted the separation at semi-preparative level of the racemic mixture **11** into the pure enantiomers *(S)*-**11** and *(R)*-**11** by chiral HPLC (Table 3). The enantiomers proved to be equipotent (EC_{50} = 0.2 nM) against the NL4-3 WT strain, and showed quite similar cytotoxic concentrations (data not shown). On the contrary, *(S)*- and *(R)*-enantiomer showed significant differences as inhibitors of the HIV-1 mutant strains. In particular, *(R)*-**11** demonstrated exceptionally antiretroviral potency against the whole viral panel, being 22- (WT, EC_{50} = 0.2 nM), 61- (K103N, EC_{50} = 2.1 nM), 6- (Y181C, EC_{50} = 933 nM) and 27-fold K103N-Y181C, EC_{50} = 150 nM), respectively, more potent than *(S)*-**11** in the cellular assay. Compound *(R)*-**11** was remarkably superior to the reference drugs NVP and EFV; with respect to AZT, *(R)*-enantiomer was superior against the WT, K103N and Y181C strains, but was 9-fold inferior against the K103N-Y181C mutant strain. Shifting the pyridinyl nitrogen atom from position 4 to either position

3 or 2 caused a marked reduction of the anti-HIV-1 activity against the mutant strains (compare **12** and **13** with **11**).

Introduction of a furanyl group for the 6-membered heterocycle led to IAS **16** which showed high antiretroviral potency against NL4-3 WT strain (EC_{50} = 0.2 nM), and the K103N (EC_{50} = 1 nM) and Y181C (EC_{50} = 4 nM) HIV-1 mutant strains, and the highest SI value (SI >282218). Unexpectedly, replacement of the furanyl group with a thiophenyl moiety (**17** and **19**) caused a reduction of the antiviral activity against the mutant viruses.

Finally, compound *(S)*-**11** and *(R)*-**11** were also evaluated against various HIV-1 group M clinical isolates in PBMC. Their antiviral activity was potent and consistent and varied only between 0.7-5.2 nM when evaluated against all different virus isolates (Table 6). Both compounds showed no activity against HIV-2 ROD in PBMC (data not shown).

Table 1. Anti-HIV-1 Activity New IASs 4-20 and Reference Compounds 1-3[a]

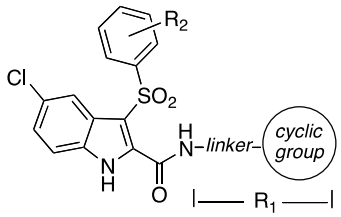

4-20

			HIV-1 NL4-3[c]			HIV-1 IIIB[e]	HIV-2 ROD[f]
compd	**R_1**	**R_2**	**CC_{50}[b] (nM)**	**EC_{50} ± SD (nM)**	**SI[d]**	**EC_{50} ± SD (nM)**	**EC_{50} (nM)**
4		3,5-Me_2	20618 ± 1053	0.23[g]	89643	nd[h]	nd
5	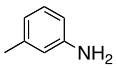	3,5-Me_2	23769 ± 5904	0.22[g]	108044	17 ± 1	nd
6		3,5-Me_2	>54953	0.22[g]	>249786	nd	nd
7	H	2,6-Me_2	>48924	44.1 ± 16.6	>1109	nd	nd
8	H	2,6-Cl_2	16017 ± 13080	0.25[g]	64068	nd	nd
9		2,6-Me_2	>55073	330.4 ± 438	>167	nd	nd
10		2,6-Cl_2	>50256	0.81 ± 0.2	>62378	nd	nd
11[i]		3,5-Me_2	30216 ± 2308	0.2 ± 0.2	151078	4.1 ± 1.3	>10000
12[i]		3,5-Me_2	54589 ± 3654	0.6[g]	90981	3.2 ± 1.3	>10000
13[i]		3,5-Me_2	54589	0.6[g]	90981	6.6 ± 0.14	>10000
14	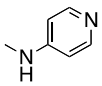	3,5-Me_2	30312 ± 1055	41.7 ± 13.1	727	730 ± 170	≥50000
15		3,5-Me_2	44105 ± 6582	2.1 ± 2.1	21002	nd	nd
16		3,5-Me_2	>56433	0.2 ± 0.1	>282218	nd	nd

17		3,5-Me_2	>54468	0.7[g]	>77812	5.2 ± 0.2	>10000[g]
18		3,5-Me_2	32346 ± 17082	0.2[g]	161730	nd	nd
19	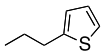	3,5-Me_2	>52853	0.84 ± 0.2	>62920	3.4 ± 1.4	>50000
20	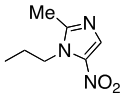	3,5-Me_2	25350 ± 1512	0.62[g]	40887	4.1 ± 1.2	>10000
1		3,5-Me_2	37994 ± 12164	0.22[g]	172700	5.7 ± 2.1	>10000[g]
2	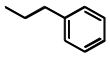	3,5-Me_2	37884 ± 15542	2.1 ± 0.9	18040	5.7 ± 1.2	>50000
3		3,5-Me_2	>53535	0.6[g]	>205903	16 ± 12	>10000
NVP	—	—	>18776	112.4 ± 74.9	>167	19.2 ± 0.0	>10000
EFV	—	—	>15839	15.9 ± 12.7	>996	1.5 ± 0.3	>10000
AZT	—	—	>30595	3.7 ± 3.7	>8269	Nd	nd

[a]Data are mean values of two to three independent experiments each one in triplicate.[b]CC_{50}: cytotoxic concentration (nM) to induce 50% death of noninfected cells, as evaluated with the MTT method in MT-4 cells. [c]EC_{50} (HIV-1 NL4−3): effective concentration (nM) to inhibit by 50% HIV-1 (NL4−3 strain) induced cell death, as evaluated with the MTT method in MT-4 cells. [d]SI: selectivity index calculated as CC_{50}/EC_{50} ratio. [e]EC_{50} (HIV-1 III_B): effective concentration (nM) or concentration required to protect CEM cells against the cytopathicity of HIV-1 (III_B strain) by 50%, as monitored by giant cell formation. [f]EC_{50} (HIV-2 ROD): effective concentration (nM) or concentration required to protect CEM cells against the cytopathicity of HIV-2 (ROD strain) by 50%, as monitored by giant cell formation. [g]Lowest detectable nM concentration. [h]nd: no data. [i]Data of R,S racemic mixture.

Table 2. Anti-HIV-1 Activity of Compounds 4-20 against Mutant HIV-1 Strains.[a,b]

	EC_{50} (nM) / FC[c]				
compd	**K103N**	**Y181C**	**Y188L**	**L100I**	**K103N-Y181C**
4	0.23[d] 1	16 ± 21 70	1273 ± 489 5535	nd[e]	>20618
5	4.4 ± 3.5 20	66 ± 66 300	947 ± 213 4305	57 ± 45 259	2137 ± 375 9714
6	0.22[d] 1	2.20 ± 1.3 10	50.6 ± 21.9 257	nd	132 ± 153 600
7	>49389 1120	42719 ± 4493 969	>48924 1110	nd	>48924 1110
8	>16018 >64072	5174 ± 1214 20696	>16018 >64072	nd	16018 ± 13080 64072
9	>55073 >167	>55073 >167	>55073 >167	nd	>55073 >167
10	5255 ± 3921 6488	2526 ± 2082 3119	>50527 >62379	nd	>50527 >62379
11[f]	9.4 ± 2.3 47	87 ± 75 435	nd	4.7 ± 3.6 24	1111 ± 940* 5555
12[f]	34 ± 13 57	230 ± 64 383	nd	45 ± 50 75	6005 ± 256 10008
13[f]	34 ± 7.1 57	220 ± 49 367	nd	20 ± 12 33	8483 ± 3633 14138
14	16000 ± 7800 384	>20000 >480	nd	nd	54953 ± 1055 1321
15	64.1 ± 42.7 31	1474 ± 940 702	>42738 >20351	nd	>42738 >20351
16	0.2[d] 1	0.8 ± 0.2 4	45 ± 0.23 225	nd	971 ± 474 4855
17	9.1 ± 2.7 13	160 ± 180 229	nd	7.1 ± 0.85 10	>54468 >77811
18	2.1 ± 1.5 11	68 ± 53 340	347 ± 217 1735	nd	2643 ± 951 13215
19	21 ± 20 25	160 ± 110 190	nd	5.4 ± 1.6 6.4	>52853 >62920
20	140 ± 71 226	670 ± 71 1081	nd	140 ± 14 226	>48452 >78148

1	0.9 ± 0.4 4	18 ± 7.0 80	90 ± 83 409	nd	1921 ± 2050 8691
2	21 ± 36 10	107 ± 107 51	>36404 >17335	19 ± 1 9	>53535 >25493
3	33 ± 6.4 55	720 ± 690 1200	nd	26 ± 24 43	3267 ± SD 5445
NVP	>3756 >33	>3756 >33	>3756 >33	60 ± 4 1.8	>3756 >33
EFV	130 ± 180 8.2	160 ± 180 10	760 ± 630 48	22 ± 14 1.4	>317 >20
AZT	16 ± 12 4.3	6.0 ± 3.4 1.6	33 ± 18 8.9	nd	16 ± 13 1.0

[a]Data are mean values of two to three independent experiments each one in triplicate. [b]EC_{50}: effective concentration (nM) to inhibit by 50% cell death induced by the indicated mutant HIV-1 strain, as evaluated with the MTT method in MT-4 cells. [c]FC: fold change obtained as ratio between EC_{50}s of the indicated drug resistant mutant HIV-1 strain and HIV-1 WT NL4-3 strain. [d]Lowest detectable nM concentration. [e]nd: no data. [f]Data of R,S racemic mixture.

Table 3. Anti-HIV-1 Activity of Racemate 11 and the Enantiomers *(S)*-11 and *(R)*-11 against Mutant HIV-1 Strains.[a,b]

	EC_{50} ± SD (nM)				
compd	**WT**	**K103N**	**Y181C**	**Y188L**	**K103N-Y181C**
11[c] *(R,S)*	0.2[d]	9.4 ± 2.3	87 ± 75	nd[fd]	1111 ± 453
11 *(S)*	0.2[d]	4.3 ± 1.7	128 ± 11	5169 ± 3160	4124 ± 913
11 *(R)*	0.2[d]	0.2[d]	2.1 ± 1.5	933 ± 38	150 ± 17
3[c,f] *(R,S)*	0.6[d]	33 ± 6.4	720 ± 690	nd[d]	26 ± 24
3[f] *(R)*	2.1 ± 1.9	4.3 ± 3.2	86 ± 43	193 ± 64	nd
3[f] *(S)*	6.3 ± 4.2	128 ± 107	3469 ± 1735	>36404	nd

[a]Data are mean values of two to three independent experiments each one in triplicate. [b]EC_{50}: effective concentration (nM) to inhibit by 50% cell death induced by the indicated mutant HIV-1 strain, as evaluated with the MTT method in MT-4 cells. [c]Data of R,S racemic mixture. [d]Lowest detectable nM concentration. [d]nd: no data. [f]Lit.[12]

Table 4. Anti-HIV-1 Activity of Compounds 5, 6 and 11-20 against the WT RT and Mutant RTs Carrying Single Amino Acid Substitutions[a]

	IC_{50} (nM)[b]			
compd	**WT**	**K103N**	**Y181I**	**L100I**
5	19	310	226	nd[c]
6	42	96	4.2	nd
11[d]	40	220	3550	30
12[d]	64	100	11100	30
13[d]	100	120	>20000	20
14	>20000	>20000	>20000	9400
15	16	234	>20000	nd
16	3	9	234	nd
17	30	>20000	>20000	100
18	27	79	nd	nd
19	70	42	>20000	1
20	44	640	131	160
1	21	>20000	>20000	15
2	77	10390	>20000	27
3	40	540	8228[c]	70
NVP	400	7000	>20000	9000
EFV	80	>20000	400	nd
ETV	10	20	164	12

[a]Data represent mean values of at least three separate experiments. [b]Compound concentration (IC_{50}, nM) required to inhibit by 50% the RT activity of the indicated strain. [c]nd, no data. [d]Data of R,S racemic mixture.

Table 5. Anti-HIV-1 Activity of Racemate 11 and its Enantiomers *(S)*-11 and *(R)*-11 against the WT RT and Mutant RTs Carrying Single Amino Acid Substitutions[a]

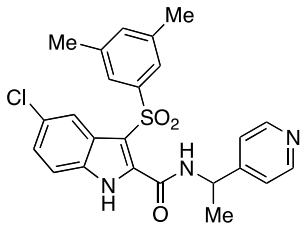

11

	IC_{50} (nM)[b]				
compd	**WT**	**K103N**	**Y181I/Y181C**[c]	**L100I**	**V106A**
11[d] *(R,S)*	40	220	3500	30	40
11 *(S)*	40	700	110000	20	55
11 *(R)*	18	50	2230	3	26
3[d,e] *(R,S)*	40	540	8228[c]	70	50
3[e] *(R)*	39	90	2531[c]	50	65
3[e] *(S)*	50	9400	>20000[c]	80	28
NVP	400	7000	>20000	9000	nd
EFV	80	>20000	400	120	nd
ETV	10	20	164	12	10

[a]Data represent mean values of at least three separate experiments. [b]Compound concentration (IC_{50}, nM) required to inhibit by 50% the RT activity of the indicated strain. [c]The recombinant HIV-1 RT carrying the Y181I mutation was comparable to the Y181C substitution in terms of drug resistance, from an enzymological point of view.[15] [d]Data of R,S racemic mixture. [e]Lit.[12]

Table 6. Inhibitory Activity of Compound *(S)*-11 and *(R)*-11 against various HIV-1 Clades Evaluated in Peripheral Blood Mononuclear Cells (PBMC).

	EC_{50} [a,b] (nM)	
HIV-1 Clade	**compd *(S)*-11**	**compd *(R)*-11**
Clade A (UG273)	5.2	3.4
Clade B (BaL)	2.0	2.1
Clade C (DJ259)	1.4	0.7
Clade D (UG270)	4.3	1.8
Clade A/E (ID12)	4.1	1.2
Clade F (BZ162)	4.9	1.6
Clade G (HH8793)	3.6	1.7

[a]Compound concentration required to inhibit HIV-1 p24 Ag production by 50% in HIV-1-infected PBMC. Data are the mean of 2 to 3 independent experiments in 2-3 different PBMC donors. [b]The clinical HIV-1 isolates were sensitive to maraviroc (CCR5 antagonist) or AMD3100 (CXCR4 antagonist) in their expected nM (1-20 nM) range.

MOLECULAR MODELING

In order to gain further insight on the binding mode of the reported compounds, a series of docking experiments was carried out following a previously reported methodology.[11a] From the docking simulations versus the HIV-1 WT RT we observed that the PLANTS proposed binding poses of IASs **4**-**20** were consistent with the one previously described for the ATIs family,[9-12] and featuring mainly by these pharmacophoric interaction: (i) the indole NH established a H-bond with the K101 carbonyl oxygen; (ii) the chlorine atom fitted into a hydrophobic cavity surrounded by V106 and L234; (iii) the

3,5-dimethylphenyl moiety lay in the aromatic cleft formed by the side chain of Y181, Y188 and W229 residues establishing a network of hydrophobic interactions; (iv) the new heteroaryl moieties formed a series of hydrophobic interactions with the side chains of V179 and E138:B. It should be noted that the extrusion of the nitrogen atom from the aromatic ring did not affect the binding mode. Interestingly, two enantiomers *(S)*-**11** and *(R)*-**11** showed an overlapping pose (Figure 2).

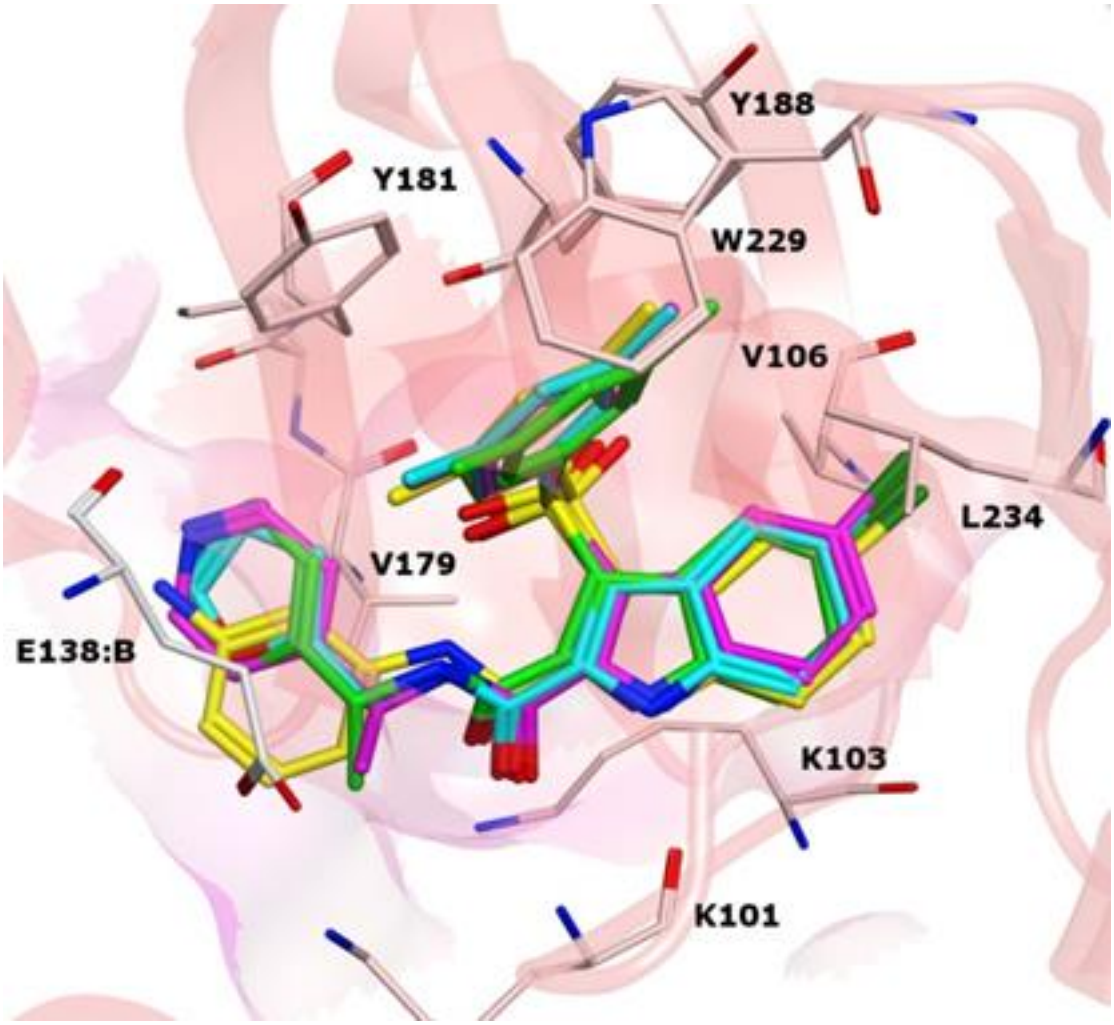

Figure 2. Binding mode of derivatives **5** (yellow), **16** (cyan), *(S)*-**11** (magenta) and *(R)*-**11** (green) into the NNBS of the WT RT. Residue of B chain is reported as white stick.

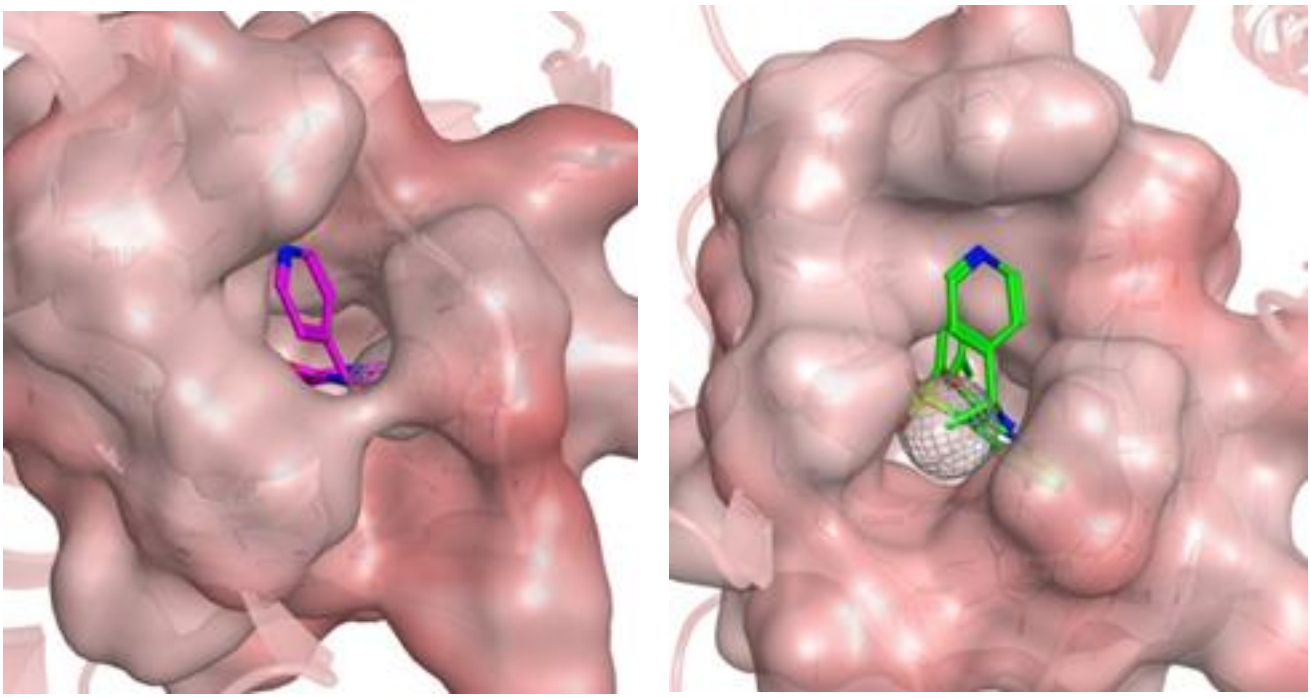

Figure 3. Binding mode of derivatives *(S)*-**11** (magenta) and *(R)*-**11** (green) into the NNBS of the K103N RT. The surfaces clearly showed the different shape and the position of the methyl group following the induced fit model.

The docking experiments were also repeated versus the K103N mutated RT. In this case, we observed that the binding mode of the majority of the compounds was not affected by the K103N mutation. However, the *(S)*- and *(R)*-enantiomers showed some significant differences in their binding mode: while the methyl group of the *(R)*-enantiomer pointed toward the cleft created by the K103N mutation, sealing the binding pocket and reducing the solvent-accessible surface, the corresponding group of the *(S)*-enantiomer left the pocket more exposed to the solvent. (Figure 3) It should be noted that this observation is in accordance with the proposed mechanism of resistance related with the K103N mutation based on a binding kinetic effect.[16,17]

To gain more information regarding the binding mode of these compounds, we performed a series of molecular dynamic simulations of both the WT and K103N mutated RT, in complex with **35** and **36**. In agreement with the biological data, the simulations into the WT RT produced very similar results for the two enantiomers. Furthermore, both complexes showed a significant stability during the whole simulation time.

In the case of the K103N RT/*(S)*-**11** and K103N RT/*(R)*-**11** complexes, the molecular dynamics trajectories analyses also showed that both complexes were stable during the whole simulation time. This is in accordance with the kinetic hypothesis of resistance, mentioned above.[16,17] Following this reasoning, the solvation effect on the protein/ligand complexes should play a major role in the binding kinetic of *(S)*-**11** and *(R)*-**11** to K103N RT. Thus, to investigate this point, we calculated the solvent accessible surface area (SASA)[18] of the binding site for both complexes during the simulations time. Interestingly, we observed a significant difference between both enantiomers; SASA of the receptor in complex with the *(S)*-enantiomer was greater than the corresponding one for the *(R)*-enantiomer, reporting values of 235.64 $Å^2$ and 210.20 $Å^2$, respectively (it should be noted that the SASA computation was performed on the entire binding site). Furthermore, we also calculated the number of water molecules inside the binding site, throughout the molecular dynamic simulation. The *(S)*-enantiomer showed a number of water molecules surrounding the methyl cleft, 3.5 times greater than the number of solvent molecules observed for the *(R)*-enantiomer. These results support our rationale and could provide a justification to the different biological activity observed with *(S)*-**11** and *(R)*-**11** (Figure 4).

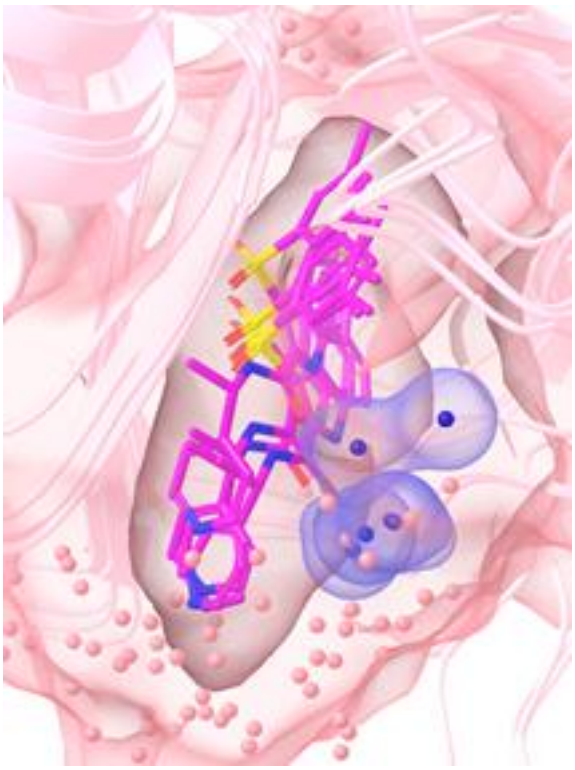

Figure 4. Four representative frames of the molecular dynamics simulation into the K103N mutated RT of the compound *(S)*-**11**. The water molecules within 6 Å from the ligand centroid are reported as blue balls; the waters beyond the binding site are reported as pink balls.

The IASs binding was thoroughly studied also in the L100I mutated RTs. This mutation seemed not to affect the binding mode of IASs **4**-**20**; the favorable interactions described above for the WT RT were still present with the L100I RT. These results are in accordance with the experimental IC_{50} values observed (*(R)*-**11**, IC_{50} WT = 18 NM and IC_{50} L100I = 3 NM). On the other hand, the docking poses observed for the Y181I RT (or Y181C RT) clearly showed the loss of the favorable π-π interaction between the 3-(3,5-dimethylphenyl) moiety and the phenyl ring of Tyr181. Also in this case the analyzed binding pose was coherent with the biological data reporting a weak enzymatic activity (*(R)*-**11**, IC_{50} Y181I = 2230 nM).

ADME Studies. Compound (*R)*-**11** (purity >99%) showed excellent plasma and metabolic stability, and did not behave as a prodrug. In the plasma stabiliy assay, (*R)*-**11** did not undergo hydrolyses for 24 h by the human plasmatic enzymes (Figure 1S, Supporting Information). The structures of the metabolites after metabolic oxidative CYP-dependent metabolism, had MW + 16 of the parent compound, in agreement with predictions #1 and #4 hypothesized by the Metasite software (Figure 2S, Supporting Information). Compound (*R)*-**11** showed good membrane permeability and low water solubility (Table 7).

Table 7. ADME Properties of Compound (*R)*-11.

Compd	PAMPA[a] Papp × 10^{-6} (cm/s)	Membrane Retention (%)	Water Solubility[b] (LogS)	Metabolic Stability[c] (%)	Major Metabolites (%)
(*R)*-11	12.4	0.0	-6.42	99.0	<0.1

[a]PAMPA: parallel artificial membrane permeability assay; [b]LogS: log mol L^{-1}; [c]% of unmodified parent drug.

CONCLUSIONS

We synthesized new indolylarylsulfone derivatives carrying a heterocyclic tail as potential anti-HIV-1/AIDS agents, with the compounds having different substituents at the indole-2-carboxamide nitrogen. Several new indolylarylsulfone (IASs) inhibited the HIV-1 WT (NL4−3 strain) in MT-4 cells with EC_{50} values in the low nanomolar range of concentration, and several compounds yielded EC_{50} values <1.0 nM and SIs >20000. Seven IASs inhibited the K103N HIV-1 mutant strain in MT-4 cells in the nanomolar range, and three of them, **4**, **6** and **16**, yielded subnanomolar EC_{50} values of 0.23, 0.22 and 0.2 nM, respectively. These compounds were also potent inhibitors of the Y181C mutation in MT-4 cells (**16**: EC_{50} = 0.8 nM). The pure enantiomers *(S)*-**11** and *(R)*-**11** obtained from the racemic **11** by

direct HPLC separation were equipotent (EC_{50} = 0.2 nM) against the NL4-3 WT strain. Most importantly, *(R)*-**11** proved to be exceptionally potent and uniformly superior to *(S)*-**11** against the whole viral panel with EC_{50} values of 0.2 nM (WT), 2.1 nM (K103N), 933 nM (Y181C) and 150 nM (K103N-Y181C) in MT-4 cells. In the RT screening assay, compound *(R)*-**11** was remarkably superior to the reference drugs NVP and EFV and comparable to ETV against the HIV-1 WT, K103N and L100I.

The binding poses of **4**-**20** were consistent with the one previously described for the IAS NNRTIs. Docking studies of the enantiomers *(S)*-**11** and *(R)*-**11** into the K103N mutated RT showed that while the methyl group of the *(R)*-enantiomer pointed toward the cleft created by the K103N mutation, the corresponding group of the *(S)*-enantiomer left the cleft more exposed to the solvent. The calculation of the solvent accessible surfaces pointed out that in the receptor complexed with the *(S)*-enantiomer this area was larger than with the *(R)*-enantiomer, accounting for the stronger inhibition of *(R)*-**11** over *(S)*-**11** against the HIV-1 K103N RT mutation.

In summary, efforts devoted to improve NNRTI activity focusing not only potency, but also aiming at more optimal resistance profile, resulted in the discovery of new valuable antiretroviral agents. Compounds **6** and **16** and the enantiomer *(R)*-**11** represent novel robust lead compounds of the IAS class that flags the direction for the development of new promising antiretroviral agents for the clinical treatment of HIV-1/AIDS.

EXPERIMENTAL SECTION

Chemistry. All reagents and solvents were commercially available and used without further purification. Organic solutions were dried over anhydrous sodium sulfate. Evaporation of the solvents was carried out on a Büchi Rotavapor R-210 equipped with a Büchi V-850 vacuum controller and Büchi V-700 (~5 mbar) and V-710 (~2 mbar) vacuum pumps. Column chromatographies were run on

glass columns packed with alumina (Merck, 70-230 mesh) or silica gel (Macherey-Nagel, 70-230 mesh) eluting with the indicated solvent. Aluminum oxide thin layer chromatography (TLC) cards from Fluka (aluminum oxide precoated aluminum cards with fluorescent indicator visualizable at 254 nm) and silica gel TLC cards from Macherey-Nagel (silica gel precoated aluminum cards with fluorescent indicator visualizable at 254 nm) were used for TLC. Developed plates were visualized by a Spectroline ENF 260C/FE UV apparatus. Melting points (mp) were determined on a SMP1 apparatus (Stuart Scientific) and are uncorrected. IR spectra were run on a SpectrumOne FT-ATR spectrophotometer (Perkin Elmer). Band position and absorption ranges are given in cm^{-1}. Proton (^1H NMR) nuclear magnetic resonance spectra were recorded on a 400 MHz FT spectrometer (Bruker) in the indicated solvent. Chemical shifts are expressed in δ units (ppm) from tetramethylsilane. Elemental analyses of tested compounds were found within 0.4% of the theoretical values. Combustion analysis was used as a method of establishing compound purity. Purity of tested compounds was ≥95%.

General Procedure for the Preparation of Derivatives 4-6 and 9-20. *Example: 5-Chloro-3-((3,5-dimethylphenyl)sulfonyl)-N-(pyridin-4-yl)-1H-indole-2-carboxamide (**4**).* A mixture of **21** (100 mg, 0.27 mmol), pyridin-4-amine (76 mg, 0.81 mmol), BOP reagent (120 mg, 0.27 mmol), and triethylamine (81 mg, 0.11 mL, 0.81 mmol) in anhydrous DMF (5 mL) was stirred at 25 °C for 12 h. The reaction mixture was diluted with water and extracted with ethyl acetate. The organic layer was washed with brine, dried and filtered. Removal of the solvent gave a residue that was purified by column chromatography (silica gel, ethyl acetate:*n*-hexane = 2:1 as eluent) to furnish **4** (17 mg, 49 %), mp 110 °C dec. (from ethanol). ^1H NMR (DMSO-d_6): δ 2.30 (s, 6H), 7.27 (s, 1H), 7.37 (d, J = 8.2 Hz, 1H), 7.58 (d, J = 8.9 Hz, 1H), 7.65 (s, 2H), 7.69 (d, J = 4.9 Hz, 2H), 7.93 (s, 1H), 8.55 (d, J = 5.6 Hz, 2H), 11.28 (s, 1H, disappeared on treatment with D_2O), 13.27 ppm (br s, 1H, disappeared on treatment with D_2O). IR: ν 1648, 2923, 2959 cm^{-1}. Anal. ($C_{22}H_{18}ClN_3O_3S$ (439.91)) C, H, Cl, N, S.

*N-(3-Aminophenyl)-5-chloro-3-((3,5-dimethylphenyl)sulfonyl)-1H-indole-2-carboxamide (**5**).* It was synthesized as **4** starting from **21** and benzene-1,3-diamine. Yield 52%, mp 218-220 °C (from ethanol). ^{1}H NMR (DMSO-d_6): δ 2.29 (s, 6H), 5.21 (br, 2H, disappeared on treatment with D_2O), 6.37 (d, *J* = 8.6 Hz, 1H), 6.80 (d, *J* = 7.6 Hz, 1H), 7.01 (t, *J* = 7.4 Hz, 1H), 7.09 (s, 1H), 7.25 (s, 1H), 7.35 (d, *J* = 8.5 Hz, 1H), 7.54 (d, *J* = 8.8 Hz, 1H), 7.64 (s, 2H), 7.92 (s, 1H), 10.60 (br s, 1H, disappeared on treatment with D_2O), 13.15 ppm (br s, 1H, disappeared on treatment with D_2O). IR: ν 1660, 3269 cm^{-1}. Anal. ($C_{23}H_{20}ClN_3O_3S$ (453.95)) C, H, Cl, N, S.

*5-Chloro-3-((3,5-dimethylphenyl)sulfonyl)-N-(pyrimidin-4-ylmethyl)-1H-indole-2-carboxamide (**6**).* It was synthesized as **4** starting from **21** and pyrimidin-4-ylmethanamine. Yield 77%, mp 225-230 °C (from ethanol). ^{1}H NMR (DMSO-d_6): δ 2.28 (s, 6H), 4.68 (d, *J* = 5.5 Hz, 2H), 7.26 (s, 1H), 7.35 (d, *J* = 8.7 Hz, 1H), 7.56 (d, *J* = 8.6 Hz, 1H), 7.67 (s, 3H), 7.94 (s, 1H), 8.81 (d, *J* = 5.2 Hz, 1H), 9.16 (s, 1H), 9.67 (br s, 1H, disappeared on treatment with D_2O), 13.13 ppm (br s, 1H, disappeared on treatment with D_2O). IR: ν 1648, 3220 cm^{-1}. Anal. ($C_{22}H_{19}ClN_4O_3S$ (454.93)) C, H, Cl, N, S.

*5-Chloro-3-((2,6-dimethylphenyl)sulfonyl)-N-(pyridin-4-ylmethyl)-1H-indole-2-carboxamide (**9**).* It was synthesized as **4** starting from **22** and pyridin-4-ylmethanamine. Yield 40%, mp 230-235 °C (from ethanol). ^{1}H NMR (DMSO-d_6): δ 2.44 (s, 6H), 4.38 (d, *J* = 5.7 Hz, 2H), 7.16 (d, *J* = 7.6 Hz, 2H), 7.26 (d, *J* = 5.2 Hz, 2H), 7.34-7.40 (m, 2H), 7.60 (d, *J* = 8.6 Hz, 1H), 7.76 (s, 1H), 8.49 (d, *J* = 5.0 Hz, 2H), 9.22 (br s, 1H, disappeared on treatment with D_2O), 13.02 ppm (br s, 1H, disappeared on treatment with D_2O). IR: ν 1638, 3251 cm^{-1}. Anal. ($C_{23}H_{20}ClN_3O_3S$ (453.94)) C, H, Cl, N, S.

*5-Chloro-3-((2,6-dichlorophenyl)sulfonyl)-N-(pyridin-4-ylmethyl)-1H-indole-2-carboxamide (**10**).* It was synthesized as **4** starting from **23** and pyridin-4-ylmethanamine. Yield 39%, mp 210-214 °C (from ethanol). ^{1}H NMR (DMSO-d_6): δ 4.48 (d, *J* = 5.8 Hz, 2H), 7.35-7.37 (m, 3H), 7.54-7.60 (m, 4H), 7.92 (s, 1H), 8.50 (d, *J* = 5.6 Hz, 2H), 9.32 (br s, 1H, disappeared on treatment with D_2O),

13.19 ppm (br s, 1H, disappeared on treatment with D_2O). IR: ν 1635, 3269, 3321 cm^{-1}. Anal. ($C_{21}H_{14}Cl_3N_3O_3S$ (494.78)) C, H, Cl, N, S.

5-Chloro-3-((3,5-dimethylphenyl)sulfonyl)-N-(1-(pyridin-4-yl)ethyl)-1H-indole-2-carboxamide ***(11).*** It was synthesized as **4** starting from **21** and 1-(pyridin-4-yl)ethanamine. Yield 71%, mp 213-216 °C (from ethanol). ^1H NMR (DMSO-d_6): δ 1.51 (d, *J* = 6.9 Hz, 3H), 2.28 (s, 6H), 5.17-5.20 (m, 1H), 7.25 (s, 1H), 7.34 (d, *J* = 8.8 Hz, 1H), 7.48 (d, *J* = 4.8 Hz, 2H), 7.54 (d, *J* = 8.7 Hz, 1H), 7.60 (s, 2H), 7.92 (s, 1H), 8.55 (d, *J* = 4.8 Hz, 2H), 9.46 (d, *J* = 6.8 Hz, 1H disappeared on treatment with D_2O), 13.04 ppm (br s, 1H, disappeared on treatment with D_2O). IR: ν 1658, 2923, 3312 cm^{-1}. Anal. ($C_{24}H_{22}ClN_3O_3S$ (467.97)) C, H, Cl, N, S.

5-Chloro-3-((3,5-dimethylphenyl)sulfonyl)-N-(1-(pyridin-2-yl)ethyl)-1H-indole-2-carboxamide ***(12).*** It was synthesized as **4** starting from **21** and 1-(pyridin-2-yl)ethanamine. Yield 43%, mp 222-225 °C (from ethanol). ^1H NMR ($CDCl_3$): δ 1.72 (d, *J* = 6.4 Hz, 3H), 2.29 (s, 6H), 5.41-5.44 (m, 1H), 7.15 (s, 1H), 7.21-7.35 (m, 4H), 7.59 (s, 2H), 7.68 (t, *J* = 7.4 Hz, 1H), 8.30 (s, 1H), 8.68 (d, *J* = 4.6 Hz, 1H), 10.28 (d, *J* = 6.8 Hz, 1H, disappeared on treatment with D_2O), 10.64 ppm (br s, 1H, disappeared on treatment with D_2O). IR: ν 1647, 3212, 3277 cm^{-1}. Anal. ($C_{24}H_{22}ClN_3O_3S$ (467.97)) C, H, Cl, N, S.

5-Chloro-3-((3,5-dimethylphenyl)sulfonyl)-N-(1-(pyridin-3-yl)ethyl)-1H-indole-2-carboxamide ***(13).*** It was synthesized as **4** starting from **21** and 1-(pyridin-3-yl)ethanamine. Yield 40%, mp 280-284 °C (from ethanol). ^1H NMR (DMSO-d_6): δ 1.54 (d, *J* = 6.8 Hz, 3H), 2.28 (s, 6H), 5.22-5.27 (m, 1H), 7.24 (s, 1H), 7.30-7.34 (m, 1H), 7.37-7.41 (m, 1H), 7.52 (d, *J* = 8.3 Hz, 1H), 7.58 (s, 2H), 7.87 (d, *J* = 7.5 Hz, 1H), 7.92 (s, 1H), 8.49 (d, *J* = 4.3 Hz, 1H), 8.70 (s, 1H), 9.43 (br s, 1H, disappeared on treatment with D_2O), 13.02 ppm (br s, 1H, disappeared on treatment with D_2O). IR: ν 1655, 2923, cm^{-1}. Anal. ($C_{24}H_{22}ClN_3O_3S$ (467.97)) C, H, Cl, N, S.

5-Chloro-3-((3,5-dimethylphenyl)sulfonyl)-N-(N'-(pyridin-4-yl)amino)-1H-indole-2-carbohydrazide ***(14).*** It was synthesized as **4** starting from **21** and 4-hydrazinylpyridine. Yield 47%, mp

231-234 °C (from ethanol). ^{1}H NMR (DMSO-d_6): δ 2.31 (s, 6H), 5.59 (br, 2H, disappeared on treatment with D_2O), 7.25 (s, 1H), 7.29 (d, *J* = 8.5 Hz, 1H), 7.52 (d, *J* = 8.4 Hz, 1H), 7.63 (s, 2H), 7.69 (s, 1H), 7.81-7.89 (m, 2H), 8.62 (d, *J* = 5.5 Hz, 2H), 12.82 ppm (br s, 1H, disappeared on treatment with D_2O). IR: ν 1689, 2923, 3554 cm^{-1}. Anal. ($C_{22}H_{19}ClN_4O_3S$ (454.93)) C, H, Cl, N, S.

5-Chloro-3-((3,5-dimethylphenyl)sulfonyl)-(N'-methylamino-N'-phenyl)-1H-indole-2-carbohydrazide ***(15)****.* It was synthesized as **4** starting from **21** and 1-methyl-1-phenylhydrazine. Yield 71%, mp 200 °C dec. (from ethanol). ^{1}H NMR (DMSO-d_6): δ 2.30 (s, 6H), 3.26 (s, 3H), 6.82 (t, *J* = 7.6 Hz, 1H), 7.04 (d, *J* = 7.3 Hz, 2H), 7.23-7.28 (m, 3H), 7.36 (d, *J* = 8.1 Hz, 1H), 7.59 (d, *J* = 8.5 Hz, 1H), 7.70 (s, 2H), 7.87 (s, 1H) 10.86 (s, 1H, disappeared on treatment with D_2O), 13.21 ppm (br s, 1H, disappeared on treatment with D_2O). IR: ν 1641, 3219 cm^{-1}. Anal. ($C_{24}H_{22}ClN_3O_3S$ (467.97)) C, H, Cl, N, S**.**

5-Chloro-3-((3,5-dimethylphenyl)sulfonyl)-N-(furan-2-ylmethyl)-1H-indole-2-carboxamide ***(16)****.* It was synthesized as **4** starting from **21** and furan-2-ylmethanamine. Yield 42%, mp 200 °C dec. (from ethanol). ^{1}H NMR (DMSO-d_6): δ 2.29 (s, 6H), 4.58 (d, *J* = 5.4 Hz, 2H), 6.45 (s, 2H), 7.25 (s, 1H), 7.33-7.35 (m, 1H), 7.53 (d, *J* = 9.0 Hz, 1H), 7.59 (s, 2H), 7.65 (s, 1H), 7.93-7.95 (m, 1H), 9.42 (br s, 1H, disappeared on treatment with D_2O), 13.05 ppm (br s, 1H, disappeared on treatment with D_2O)). IR: ν 1637, 3210 cm^{-1}. Anal. ($C_{22}H_{19}ClN_2O_4S$ (442.92)) C, H, Cl, N, S**.**

5-Chloro-3-((3,5-dimethylphenyl)sulfonyl)-N-(thiophen-2-ylmethyl)-1H-indole-2-carboxamide ***(17)****.* It was synthesized as **4** starting from **21** and thiophen-2-ylmethanamine. Yield 73%, mp 252-255 °C (from ethanol). ^{1}H NMR (DMSO-d_6): δ 2.27 (s, 6H), 4.75 (d, *J* = 5.6 Hz, 2H), 7.00-7.03 (m, 1H), 7.15-7.16 (m, 1H), 7.25 (s, 1H), 7.33 (d, *J* = 8.8 Hz, 1H), 7.46 (d, *J* = 4.9 Hz, 1H), 7.53 (d, *J* = 8.5 Hz, 1H), 7.58 (s, 2H), 7.95 (s, 1H) 9.51 (br s, 1H, disappeared on treatment with D_2O), 13.07 ppm (br s, 1H, disappeared on treatment with D_2O)). IR: ν 1647, 2922, 3231 cm^{-1}. Anal. ($C_{22}H_{19}ClN_2O_3S_2$ (458.98)) C, H, Cl, N, S.

*5-Chloro-3-((3,5-dimethylphenyl)sulfonyl)-N-(1-(thiophen-2-yl)ethyl)-1H-indole-2-carboxamide (**18**).* It was synthesized as **4** starting from **21** and 1-(thiophen-2-yl)ethanamine. Yield 41%, mp 215-217 °C (from ethanol). ^{1}H NMR (DMSO-d_6): δ 1.62 (d, J = 6.8 Hz, 3H), 2.28 (s, 6H), 5.44-5.50 (m, 1H), 7.00-7.03 (m, 1H), 7.16-7.17 (m, 1H), 7.26 (s, 1H), 7.34 (d, J = 8.4 Hz, 1H), 7.46 (d, J = 5.0 Hz, 1H), 7.54 (d, J = 8.6 Hz, 1H), 7.58 (s, 2H), 7.94 (s, 1H) 9.48 (d, J = 7.9 Hz, 1H, disappeared on treatment with D_2O), 13.03 ppm (br s, 1H, disappeared on treatment with D_2O)). IR: ν 1644, 3238 cm^{-1}. Anal. ($C_{23}H_{21}ClN_2O_3S_2$ (473.01)) C, H, Cl, N, S.

*5-Chloro-3-((3,5-dimethylphenyl)sulfonyl)-N-(2-(thiophen-2-yl)ethyl)-1H-indole-2-carboxamide (**19**).* It was synthesized as **4** starting from **21** and 2-(thiophen-2-yl)ethanamine. Yield 82%, mp 222-224 °C (from ethanol). ^{1}H NMR (DMSO-d_6): δ 2.31 (s, 6H), 3.09-3.17 (m, 2H), 3.58-3.68 (m, 2H), 6.96-7.00 (m, 2H), 7.26 (s, 1H), 7.32-7.39 (m, 2H), 7.52-7.57 (m, 1H), 7.62 (s, 2H), 7.93 (d, J = 3.3 Hz, 1H), 9.17 (br s, 1H, disappeared on treatment with D_2O), 13.05 ppm (br s, 1H, disappeared on treatment with D_2O)). IR: ν 1652, 2854, 3238 cm^{-1}. Anal. ($C_{23}H_{21}ClN_2O_3S_2$ (473.01)) C, H, Cl, N, S.

*5-Chloro-3-((3,5-dimethylphenyl)sulfonyl)-N-(2-(2-methyl-5-nitro-1H-imidazol-1-yl)ethyl)-1H-indole-2-carboxamide (**20**).* It was synthesized as **4** starting from **21** and 2-(2-methyl-5-nitro-1*H*-imidazol-1-yl)ethanamine. Yield 78%, mp 232-234 °C (from ethanol). ^{1}H NMR (DMSO-d_6): δ 2.32 (s, 6H), 2.49 (s, 3H), 3.74-3.77 (m, 2H), 4.48-4.54 (m, 2H), 7.27 (s, 1H), 7.32-7.38 (m, 1H), 7.52-7.56 (m, 1H), 7.63 (s, 2H), 7.92 (d, J = 3.0 Hz, 1H), 8.06 (s, 1H), 9.23 (br s, 1H, disappeared on treatment with D_2O), 12.89 ppm (br s, 1H, disappeared on treatment with D_2O)). IR: ν 1600, 2933 cm^{-1}. Anal. ($C_{23}H_{22}ClN_5O_5S$ (515.97)) C, H, Cl, N, S.

General Procedure for the Preparation of Derivatives 7 and 8. *Example: 5-Chloro-3-((2,6-dimethylphenyl)sulfonyl)-1H-indole-2-carboxamide (**7**).* 30% Ammonium hydroxide (6.5 mL) was added to a suspension of **29** (110 mg, 0.28 mmol) in ethanol (11 mL). The reaction mixture was stirred

for 30 minutes at 60 °C, then 30% ammonium hydroxide (6.5 mL) was added again and the reaction was heated at 60 °C overnight. After cooling, the mixture was diluted with water and extracted with ethyl acetate. The organic layer was washed with brine, dried and filtered. Removal of the solvent gave a residue that was purified by column chromatography (silica gel, ethyl acetate as eluent) to furnish **7** (30 mg, 35 %), mp 265-270 °C (from ethanol). ^{1}H NMR (DMSO-d_6): δ 2.46 (s, 6H), 7.18-7.20 (m, 2H), 7.32-7.40 (m, 2H), 7.68 (d, *J* = 8.9 Hz, 1H), 7.69-7.71 (m, 1H), 8.08 (br s, 2H, disappeared on treatment with D_2O), 12.94 ppm (br s, 1H, disappeared on treatment with D_2O). IR: ν 1648, 3227 cm^{-1}. Anal. ($C_{17}H_{15}ClN_2O_3S$ (362.83)) C, H, Cl, N, S.

*5-Chloro-3-((2,6-dichlorophenyl)sulfonyl)-1H-indole-2-carboxamide (**8**).* It was synthesized as **7** starting from **30** (yield 32%). Spectral and chemico-physical data were in agreement with those previously reported.[9b]

General Procedure for the Preparation of Derivatives 25 and 26. *Example: 5-Chloro-3-((2,6-dimethylphenyl)thio)-1H-indole-2-carboxylic acid (**25**).* To a mixture of NaH (60 % in mineral oil) (220 mg, 5 mmol) in anhydrous DMF (7 mL) was added **24** (450 mg, 2.3 mmol) and the reaction mixture was stirred at 25 °C for 10 minutes. 1,2-Bis-(2,6-dimethylphenyl)disulfide (700 mg, 2.5 mmol) was added and the reaction mixture was stirred at 100 °C overnight. The reaction mixture was diluted with water, made acid with 6N HCl, and extracted with ethyl acetate. The organic layer was washed with brine, dried and filtered. Removal of the solvent gave the crude acid that was used without further purification.

*5-Chloro-3-((2,6-dimethylphenyl)thio)-1H-indole-2-carboxylic acid (**26**).* It was synthesized as **25** starting from **24** and 1,2-bis-(2,6-dichlorophenyl)disulfide. It was used as crude product without further purification.

General Procedure for the Preparation of Derivatives 27 and 28. *Example: Ethyl 5-chloro-3-((2,6-dimethylphenyl)thio)-1H-indole-2-carboxylate (**27**).* Thionyl chloride (1.8 g, 1.07 mL, 15

mmol) was added dropwise to a mixture of **25** in anhydrous ethanol (16 mL, 280 mmol), and the reaction was heated at reflux overnight. After cooling the mixture was diluted with water and extracted with ethyl acetate. The organic layer was washed with brine, dried and filtered. Removal of the solvent gave a residue that was purified by column chromatography (silica gel, ethyl acetate:*n*-hexane = 1:3 as eluent) to furnish **27** (220 mg, 51 %), mp 180-185 °C (from ethanol). ^{1}H NMR (DMSO-d_6): δ 1.36 (t, *J* = 5.2 Hz, 3H), 2.32 (s, 6H), 4.36-4.42 (m, 2H), 6.41-6.43 (m, 1H), 7.17-7.20 (m, 3H), 7.25-7.27 (m, 1H), 7.42-7.46 (m, 1H), 12.17 ppm (br s, 1H, disappeared on treatment with D_2O). IR: ν 1671, 3313 cm^{-1}.

*Ethyl 5-chloro-3-((2,6-dichlorophenyl)thio)-1H-indole-2-carboxylate (**28**).* It was synthesized as **27** starting from **26**. Yield 62%, mp 208-211 °C (from ethanol). ^{1}H NMR (DMSO-d_6): δ 1.32 (t, *J* = 7.1 Hz, 3H), 4.36-4.39 (m, 2H), 6.89 (s, 1H), 7.25 (d, *J* = 8.8 Hz, 1H), 7.39-7.48 (m, 2H), 7.55-7.57 (m, 2H), 12.39 ppm (br s, 1H, disappeared on treatment with D_2O). IR: ν 1671, 3296 cm^{-1}.

General Procedure for the Preparation of Derivatives 29 and 30. *Example: ethyl 5-chloro-3-((2,6-dimethylphenyl)sulfonyl)-1H-indole-2-carboxylate (**29**).* MCPBA (274 mg, 1.2 mmol) was added portionwise to a mixture of **27** (220 mg, 0.61 mmol) in chloroform (20 mL) at 0 °C. The reaction mixture was stirred at room temperature for 2 h. Water was added and the mixture was extracted with chloroform. The organic layer was washed with brine, dried and filtered. Removal of the solvent gave a residue that was purified by column chromatography (silica gel, ethyl acetate:*n*-hexane = 1:2 as eluent) to furnish **29** (180 mg, 75 %), mp 190-192 °C (from ethanol). ^{1}H NMR (DMSO-d_6): δ 1.10 (t, *J* = 5.5 Hz, 3H), 2.43 (s, 6H), 4.11-4.16 (m, 2H), 7.16 (d, *J* = 6.8 Hz, 2H), 7.36 (t, *J* = 8.6 Hz, 1H), 7.42-7.46 (m, 1H), 7.62-7.65 (m, 1H), 8.23-8.25 (m, 1H), 13.26 ppm (br s, 1H, disappeared on treatment with D_2O). IR: ν 1727, 3360 cm^{-1}.

*Ethyl 5-chloro-3-((2,6-dichlorophenyl)sulfonyl)-1H-indole-2-carboxylate (**30**).* It was synthesized as **29** starting from **28**. Yield 67%, mp 270-272 °C (from ethanol). ^{1}H NMR (DMSO-d_6): δ

1.12 (t, *J* = 7.2 Hz, 3H), 4.17-4.22 (m, 2H), 7.44-7.48 (m, 1H), 7.56-7.65 (m, 4H), 8.19-8.21 (m, 1H), 13.35 ppm (br s, 1H, disappeared on treatment with D_2O). IR: ν 1722, 3266 cm^{-1}.

General Procedure for the Preparation of Derivatives 22 and 23. *Example: 5-chloro-3-((2,6-dimethylphenyl)sulfonyl)-1H-indole-2-carboxylic acid (**23**).* Lithium hydroxide monohydrate (50 mg, 1.2 mmol) was added to a solution of **27** (180 mg, 0.4 mmol) in THF (5 mL) and water (5 mL). Then the reaction mixture was stirred at room temperature for 48 h. After dilution with water, the mixture was treated with 1 N HCl until pH 2 was reached. The acid was extracted with ethyl acetate, washed with brine, dried and filtered. Removal of the solvent gave a residue that was purified by column chromatography (silica gel, chloroform:ethanol = 7:3 as eluent) to furnish **22** (140 mg, 96 %), mp 280-285 °C (from ethanol). ^{1}H NMR (DMSO-d_6): δ 2.46 (s, 6H), 7.05 (d, *J* = 7.3 Hz, 2H), 7.23 (t, *J* = 8.6 Hz, 2H), 7.55-7.57 (m, 1H), 8.19 (s, 1H), 12.20 ppm (br s, 1H, disappeared on treatment with D_2O) IR: ν 1726, 2924, 3358 cm^{-1}.

*5-Chloro-3-((2,6-dichlorophenyl)sulfonyl)-1H-indole-2-carboxylic acid (**23**).* It was synthesized as **22** starting from **30**. Yield 85%, mp 199-202 °C (from ethanol). ^{1}H NMR (DMSO-d_6): δ 7.23 (d, *J* = 8.0 Hz, 1H), 7.38-7.46 (m, 3H), 7.55-7.60 (m, 1H), 8.10 (s, 1H), 12.54 ppm (br s, 1H, disappeared on treatment with D_2O). IR: ν 1611, 3213 cm^{-1}.

General Procedure for the Preparation of Derivatives 33 and 34. *Example: 1,2-bis(2,6-dimethylphenyl)disulfide (**33**).* 1,3-Dibromo-5,5-dimethylhydantoin (500 mg, 1.8 mmol) was added to a mixture of 2,6-dimehylthiophenol (1.0 g, 7.2 mmol, 0.96 mL) in chloroform (15 mL) at room temperature. The reaction mixture stirred at 25 °C for 5 minutes. Saturated solution of potassium carbonate was added; the mixture was made acidic to pH 2 with 1 N HCl and extracted with chloroform, washed with brine and dried. Removal of the solvent gave a residue that was purified by column chromatography (silica gel, petroleum ether:dichloromethane = 7:3 as eluent) to furnish **33** (620 mg, 99 %), mp 90-94 °C (from ethanol) (Lit.[19] 99-102°C).

*1,2-Bis(2,6-dichlorophenyl)disulfide (**34**).* It was synthesized as **33** starting from **32**. Yield 91%, yellow solid, mp 202-205 °C (from ethanol) (Lit.[20] 196 °C).

Separation of Racemate 11 into the Enantiomers (*S*)-11 and (*R*)-11. HPLC enantioseparations were performed by using the stainless-steel Chiralcel OD (250 mm x 4.6 mm i.d. and 250 x 10 mm i.d.) (Chiral Technologies Europe, Illkirch, France) columns. All chemicals solvents for HPLC were purchased from Aldrich (Italy) and used without further purification. The analytical HPLC apparatus consisted of a Perkin-Elmer (Norwalk, CT, USA) 200 lc pump equipped with a Rheodyne (Cotati, CA, USA) injector, a 20-μL sample loop, a HPLC Dionex CC-100 oven (Sunnyvale, CA, USA) and a Jasco (Jasco, Tokyo, Japan) Model CD 2095 Plus UV/CD detector. For semipreparative separations a Perkin-Elmer 200 LC pump equipped with a Rheodyne injector, a 1 mL sample loop, a Perkin-Elmer LC 101 oven and Waters 484 detector (Waters Corporation, Milford, MA, USA) were used. The signal was acquired and processed by Clarity software (DataApex, Prague, The Czech Republic). The circular dichroism (CD) spectra were measured by using a Jasco Model J-700 spectropolarimeter. The optical path and temperature were set at 0.1 mm and 20 °C, respectively. The spectra are average computed over three instrumental scans and the intensities are presented in terms of ellipticity values (mdeg).

Biological Assays. *Inhibition of HIV-induced cytopathicity*. Biological activity of the compounds was tested in the lymphoid MT-4 cell line (received from the NIH AIDS Reagent Program) against the WT HIV-1 NL4-3 strain and the different mutant HIV-1 strains, as described before.[21] Briefly, MT-4 cells were infected with the appropriate HIV-1 strain (or mock-infected to determine cytotoxicity) in the presence of different drug concentrations. At day five post-infection, a tetrazolium-based colorimetric method (MTT method) was used to evaluate the number of viable cells. The methodology for the anti-HIV assays in CEM cells had been described previously.[22] Briefly, human CEM cell cultures (~3 x 10^5

cells/mL^{-1}) were infected with ~100 $CCID_{50}$ HIV-1 IIIB or HIV-2 ROD per mL and seeded in 200 µL-well microtiter plates, containing appropriate dilutions of the test compounds. After 4 days of incubation at 37 °C, syncytia cell formation was examined microscopically in the CEM cell cultures.

Enzymatic assay procedures. Chemicals. [^{3}H]dTTP (40 Ci/mmol) was from Amersham and unlabelled dNTP's from Boehringer. Whatman was the supplier of the GF/C filters. All other reagents were of analytical grade and purchased from Merck or Fluka. The homopolymer poly(rA) (Pharmacia) was mixed at weight ratios in nucleotides of 10:1, to the oligomer oligo$(dT)_{12-18}$ (Pharmacia) in 20 mM Tris-HCl (pH 8.0), containing 20 mM KCl and 1 mM EDTA, heated at 65 °C for 5 min and then slowly cooled at room temperature. The coexpression vectors pUC12N/p66(His)/p51with the wild-type or the mutant forms of HIV-1 RT p66 were kindly provided by Dr. S. H. Hughes (NCI-Frederick Cancer Research and Development Center). Proteins were expressed in *E. coli* and purified as described.[23] RNA-dependent DNA polymerase activity was assayed as follows: a final volume of 25 µL contained reaction buffer (50 mM Tris-HCl pH 7.5, 1 mM DTT, 0.2 mg/mL BSA, 4% glycerol), 10 mM $MgCl_2$, 0.5 µg of poly(rA)/oligo$(dT)_{10:1}$ (0.3 µM 3'-OH ends), 10 µM [3H]-dTTP (1Ci/mmol) and 2-4 nM RT. Reactions were incubated at 37 °C for the indicated time. 20 µL-Aliquots were then spotted on glass fiber filters GF/C which were immediately immersed in 5% ice-cold TCA. Filters were washed twice in 5% ice-cold TCA and once in ethanol for 5 min, dried and acid-precipitable radioactivity was quantitated by scintillation counting. Reactions were performed under the conditions described for the HIV-1 RT RNA-dependent DNA polymerase activity assay. Incorporation of radioactive dTTP into poly(rA)/oligo(dT) at different substrate (nucleic acid or dTTP) concentrations was monitored in the presence of increasing fixed amounts of inhibitor. Data were then plotted according to Lineweaver-Burke and Dixon. For K_i determination, an interval of inhibitor concentrations between 0.2 K_i and 5 K_i was used.

Inhibition of HIV-1 clades. Inhibition of various HIV-1 clades (group M) was evaluated in PBMC. PBMCs from healthy donors were stimulated with PHA at 2 µg/mL (Sigma, Bornem, Belgium) for 3 days at 37 °C. The PHA-stimulated blasts were then seeded at 0.5 x 106 cells per well into a 48-well plate containing varying concentrations of compound in cell culture medium (RPMI 1640) containing 10% FCS and IL-2 (25 U/mL, R&D Systems Europe, Abingdon, UK). The virus stocks were added at a final dose of 250 pg p24 or p27/mL. The primary clinical isolates representing different HIV-1 clades of group M and an HIV-2 isolate were all kindly provided by Dr. J. Lathey then at BBI Biotech Research Laboratories, Inc., Gaithersburg, MD, and their co-receptor use (R5 or X4) was determined in our laboratory in U87.CD4.CXCR4 and U87.CD4.CCR5 cells. Cell supernatant was collected at day 10-12 after infection and HIV-1 core Ag in the culture supernatant was analyzed by a p24 Ag ELISA kit (Perkin Elmer, Zaventem, Belgium). For HIV-2 p27 Ag detection the INNOTEST from Innogenetics (Temse, Belgium) was used.[24]

Molecular Modeling. All molecular modeling studies were performed on a Intel® Xeon(R) CPU E5462 2.80 GHz x 4 running Ubuntu 12.04 LTS. The RT structures were downloaded from the PDB (WT RTs: 2rf2[15], K103N RT: 1fk0,[25] L100I RT: 1S1T RT,[26] the Y181I mutation was obtained by mutating the specific residue in the 1jkh[27] crystal using the rotamer explorer tool in MOE and using the lowest energy conformation obtained. Hydrogen atoms were added to the protein using Molecular Operating Environment (MOE) 2010.10[28] and minimized, keeping all the heavy atoms fixed until a rmsd gradient of 0.05 kcal mol^{-1} $Å^{-1}$ was reached. Ligand structures were built with MOE and minimized using the MMFF94x force field until a rmsd gradient of 0.05 kcal mol^{-1} $Å^{-1}$ was reached. The docking simulations were performed using PLANTS 1.1.[29] We set the binding lattice as a sphere of 10 Å binding site radius from the center of WT and mutated RT co-crystallized inhibitor. All Molecular Dynamics (MD) simulations were performed on Desmond package of Maestro

SCHRÖDINGER 2.4,[30,31] using OPLS all-atom force field 2005.[32,33] All protein complex system for MD simulations were prepared by Desmond set up wizard. The complexes were solvated in a periodic octahedron simulation box using TIP3P water molecules, providing a minimum of 10 Å of water between the protein surface and any periodic box edge. Chlorine ions were added to neutralize the charge of the total system.

The systems were equilibrated with the default protocol provided in Desmond. Two rounds of steepest descent were performed with a maximum of 2000 steps on a restraint of 50 kcal/mol per $Å^2$. Then, a serie of four molecular dynamic equilibrations were performed. The first simulation was run for 12 ps at a temperature of 10 °K in the NVT ensemble with proteins and ligands heavy atoms restrained with force constant of 50 kcal/mol per $Å^2$. Another 12 ps simulation was performed with the same harmonic restraints; this time in the NPT ensemble. A 24-ps simulation followed with the temperature raised to performed at 300 °K in the NPT ensemble and the force constant retained. Finally, a 24-ps simulation was performed at 300 °K in the NPT ensemble with all restraints removed. Following minimization, the entire system was heated to 300 °K with constant pressure of 1.013 bar and periodic boundary condition for 20 ns. Trajectories analysis were carried out by Simulation Integrations Diagram of Desmond application. SASA was computed every ten frames in each step and the binding cavity of the protein was defined by a 5 Å radius from the bound ligand, using a python script developed by Schrödinger. The computation of the water molecules inside the binding site was determined by counting the water molecules within a specified distance of 6 Å from the ligand centroid. The images in the manuscript were created with MOE 2010.10 and Maestro SCHRÖDINGER 2.4.

Purity determination. Compound (*R*)-**11** was dissolved in DMSO (1 mM) and analysed by LC-UV-MS chromatography. LC analysis were performed with an Agilent 1100 LC/MSD VL system

(G1946C) (Agilent Technologies, Palo Alto, CA) equipped with vacuum solvent degassing unit, binary high-pressure gradient pump, 1100 series UV detector, and 1100 MSD model VL bench top mass spectrometer. Chromatographic profiles were obtained using a Kinetex C18 column (Phenomenex, 100 x 4.6 mm, 2.6 μm particle size, and gradient elution: eluent A = ACN, eluent B = water. The analysis started with 2% of A, which rapidly increased up to 70% in 12 min and then slowly up to 98% in 20 min. The flow rate was 0.4 mL min^{-1} and injection volume was 20 μL.

The Agilent 1100 series mass spectra detection (MSD) single-quadrupole instrument carried an orthogonal spray API-ES (Agilent Technologies, Palo Alto, CA). Nitrogen was used as nebulizing and drying gas. The pressure of the nebulizing gas, flow of the drying gas, capillary voltage, fragmentor voltage, and vaporization temperature were set at 40 psi, 9 L/min, 3000 V, 70 V, and 350 °C, respectively. UV detection was monitored at 254 nm. The LC-ESI-MS determination was performed by operating the MSD in the positive ion mode. Spectra were acquired over the scan range *m/z* 100-1500 using a step size of 0.1 μ. The compound purity was determined by measuring the peak areas detected at 254 nm.

Water Solubility Assay. Compound (*R*)-**11** (1 mg) was added as a powder to 1 mL of water. The mixture was stirred at room temperature for 24 h. The suspension was taken off by a 0.45 μm nylon filter (Acrodisc), and the solubilized compound was determined by LC-UV-MS assay. The experiments were carried out in triplicate. The quantification was performed with ES interface and Varian MS Workstation System Control Vers. 6.9 software. Chromatographic analysis was carried out as above reported; gradient elution: eluent A = ACN, eluent B = water containing 0.1% formic acid. The analysis started with 0% of A, which linearly increased up to 70% in 10 min and then slowly up to 98% in 15 min. The flow rate was 0.2 mL min^{-1} and injection volume was 5 μL. The instrument operated in positive mode with detector 1850 V, drying gas pressure 25.0 psi, desolvation temperature 300 °C, nebulizing gas 40 psi, needle 5000 V and shield 600 V. Nitrogen was used as nebulizer gas

and drying gas. Collision induced dissociation was performed using Argon as the collision gas at a pressure of 1.8 mTorr in the collision cell. The transitions as well as the capillary voltage and the collision energy used for compound are summarized in Table 8.

Table 8. Chromatographic and MS Parameters of Compound (*R*)-11.

Compd	Transition[a] (m/z)	Collision Energy (eV)	Capillary Voltage (V)	t_R[b] (min)
(*R*)-11	348.8 105.8	-24.0 -22.5	18	99.0

[a]monitored transition; [b]retention time.

Parallel Artificial Membrane Permeability Assay (PAMPA). Donor solution of compound (*R*)-**11** (0.5 mM) was prepared by diluting 1 mM DMSO stock solution with phosphate buffer (pH 7.4, 25 mM). Filters were coated with 5 □L of a 1% (w/v) dodecane solution of phosphatidylcholine for intestinal permeability. The donor solution (150 μL) was added to each well of the filter plate. To each well of the acceptor plate were added 300 μL of 50% DMSO - phosphate buffer solution. The experiments were carried out in three plates on different days. The sandwich was incubated for 5 h at room temperature under gentle shaking. After incubation, the plates were separated, and samples were taken from both receiver and donor sides and analysed using LC with UV detection at 254 nm. LC analysis were performed with a Perkin-Elmer series 200 provided with an UV detector (Perkin-Elmer 785A, UV/vis Detector). Chromatographic separations were achieved using a Kinetix C18 column (Phenomenex, 100 x 4.6 mm, 2.6 μm particle size at a flow rate of 0.6 mL min^{-1} and a mobile phase of 6:4 ACN-water.

Permeability (P_{app}) for PAMPA was calculated according to the following equation, obtained from Wohnsland and Faller,[34] and Sugano et al.[35] and modified in order to obtain permeability values in cm/s,

$$P_{app} = \frac{V_D V_A}{(V_D + V_A)At} - \ln(1 - r)$$

where V_A is the volume in the acceptor well, V_D is the volume in the donor well (cm^3), A is the effective area of the membrane (cm^2), t is the incubation time (s) and r the ratio between drug concentration in the acceptor and equilibrium concentration of the drug in the total volume (V_D+V_A). Drug concentration is estimated by using the peak area integration.

Membrane retention (%) was calculated according to the following equation:

$$\%MR = \frac{[r - (D + A)]100}{Eq}$$

where r is the ratio between drug concentration in the acceptor and equilibrium concentration, D, A, and Eq represent drug concentration in the donor, acceptor and equilibrium solution, respectively.

Microsomal Stability Assay. Compound (*R*)-**11** in DMSO solution was incubated at 37 °C for 60 min in 25 mM phosphate buffer (pH 7.4), 5 μL of human liver microsomal protein (0.2 mg/mL), in the presence of a NADPH-generating system at a final volume of 0.5 mL and concentration of 50 μM; DMSO did not exceed 2%. The reaction was cooled on ice and quenched by adding 1.0 mL of ACN. The reaction mixtures were centrifuged for 15 min at 10000 rpm, and the parent drug and its metabolites were determined by LC-UV-MS. The chromatographic analysis was performed as above reported. The percentage of unmetabolized compound was calculated using reference solutions. The experiments were performed in triplicate and the metabolic behaviour was predicted by means of Metasite software.

Plasma Stability Assay. To determine the enzymatic stability, pooled human plasma (750 μL), phosphate buffer (pH 7.4, 700 μL), and 50 μL of 3.0 mM solution of (*R*)-**11** in DMSO (final

concentration 100 µM) were mixed in a test tube. The mixture was incubated at 37 °C. At the time points of 0 h and 24 h aliquots of a 150 µL were removed, mixed with 600 µL of cold ACN and centrifuged at 5000 rpm for 15 min. The supernatant was removed and analysed by HPLC. The stability was checked by HPLC with UV-MS detector as above reported.

ASSOCIATED CONTENT

Supporting Information

Additional chemical and biological material is available free of charge via the internet at http//pubs.acs.org.

AUTHOR INFORMATION

Corresponding Authors

*Phone: +39 06 4991 3404. Fax: +39 06 4991 39933. E-mail: giuseppe.laregina@uniroma1.it.

Notes

The authors declare no competing financial interest.

ACKNOWLEDGMENTS

The authors would like to thank S. Claes, E. Van Kerckhove and E. Fonteyn for excellent technical assistance. This work, in part, was supported by funding of the Istituto Pasteur - Fondazione Cenci Bolognetti, K.U. Leuven (GOA 10/014 and PF/10/018), the Foundation of Scientific Research (FWO no. G-0485-08 and G-0528-12) and the Spanish MINECO (project BFU2012-31569).

ABBREVIATIONS USED

IAS, indolylarylsulfone; HIV-1, human immunodeficiency virus type 1; AIDS, acquired immunodeficiency syndrome; RT, reverse transcriptase; NRTI, nucleoside reverse transcriptase inhibitor; NNRTI, non-nucleoside reverse transcriptase inhibitor; ART, antiretroviral therapy; HAART, highly active antiretroviral therapy; DADS, diaryldisulfide; WT, wilde type; NVP, nevirapine; EFV, efavirenz; ETV, etravirine; CEM cells, human T-lymphocyte cells; SASA, solvent accessible surface area.

References

(1) Lafemina, R. Human immunodeficiency virus type I non-nucleoside reverse transcriptase inhibitors. In *Antiviral Research: Strategies in Antiviral Drug Discovery*, ASM Press, Washington, 2009, pp 33–50.

(2) Virgin, H. W.; Walker, B. D. Immunology and the elusive AIDS vaccine. *Nature* **2011**, *464*, 224–231.

(3) Global report: UNAIDS report on the global AIDS epidemic 2013. http://www.unaids.org/en/resources/campaigns/globalreport2013/globalreport/.

(4) Antiretroviral drugs used in the treatment of HIV infection, FDA, Last Updated: 08/20/2013.

(5) Este, J. A.; Cihlar, T. Current status and challenges of antiretroviral research and therapy. *Antiviral Res.* **2010**, *85*, 25–33.

(6) Menendez-Arias, L. Molecular basis of human immunodeficiency virus type 1 drug resistance: overview and recent developments. *Antiviral Res* **2013,** 98, 93–120.

(7) Grant, P. M.; Zolpa, A. R. Optimal antiretroviral therapy: HIV-1 treatment strategies to avoid and overcome drug resistance. *Curr. Opin. Investig. Drugs* **2010**, 11, 901–910.

(8) (a) Cortez, K. J.; Maldarelli, F. Clinical management of HIV drug resistance. *Viruses* **2011**, *3*, 347-378; (b) Hawkins, T. Understanding and managing the adverse effects of antiretroviral therapy. *Antiviral Res*. **2010**, *85*, 201–209.

(9) (a) Silvestri, R.; De Martino, G.; La Regina, G.; Artico, M.; Massa, S.; Vargiu, L.; Mura, M.; Loi, A. G.; Marceddu, T.; La Colla, P. Novel indolyl aryl sulfones active against HIV-1 carrying NNRTI resistance mutations: synthesis and SAR studies. *J. Med. Chem.* **2003**, *46*, 2482–2493; (b) Silvestri, R.; Artico, M.; De Martino, G.; La Regina, G.; Loddo, R.; La Colla, M.; La Colla, P. Simple, short peptide derivatives of a sulfonylindolecarboxamide (L-737,126) active in vitro against HIV-1 wild-type and variants carrying non-nucleoside reverse transcriptase inhibitor resistance mutations. *J. Med. Chem.* **2004**, *47*, 3892–3896; (c) Piscitelli, F.; Coluccia, A.; Brancale, A.; La Regina, G.; Sansone, A.; Giordano, C.; Balzarini, J.; Maga, G.; Zanoli, S.; Samuele, A.; Cirilli, R.; La Torre, F.; Lavecchia, A.; Novellino, E.; Silvestri, R. Indolylarylsulfones bearing natural and unnatural amino acids. Discovery of potent inhibitors of HIV-1 non-nucleoside wild type and resistant mutant strains reverse transcriptase and Coxsackie B4 virus. *J. Med. Chem.* **2009**, *52*, 1922−1934. (d) Ragno, R.; Artico, M.; De Martino, G.; La Regina, G.; Coluccia, A.; Di Pasquali, A.; Silvestri, R. Docking and 3-D QSAR studies on indolyl aryl sulfones (IASs). Binding mode exploration at the HIV-1 reverse transcriptase non-nucleoside binding site and design of highly active *N*-(2-hydroxyethyl)carboxyamide and *N*-(2-hydroxyethyl)-carboxyhydrazide derivatives. *J. Med. Chem.* **2005**, *48*, 213−223; (e) Ragno, R.; Coluccia, A.; La Regina, G.; De Martino, G.; Piscitelli, F.; Lavecchia, A.; Novellino, E.; Bergamini, A.; Ciaprini, C.; Sinistro, A.; Maga, G.; Crespan, E.; Artico, M.; Silvestri, R. Design, molecular modeling, synthesis and anti-HIV-1

activity of new indolyl aryl sulfones. Novel derivatives of the indole-2-carboxamide. *J. Med. Chem.* **2006**, *49*, 3172−3184.

(10) (a) La Regina, G.; Coluccia, A.; Silvestri, R. Looking for an active conformation of the future HIV-1 non-nucleoside reverse transcriptase inhibitors. *Antiviral Chem. Chemoth.* **2010**, *20*, 231–237; (b) Chong, P.; Sebahar, P.; Youngman, M.; Garrido, D.; Zhang, H.; Stewart, E. L.; Nolte, R. T.; Wang, L.; Ferris, R. G.; Edelstein, M.; Weaver, K.; Mathis, A.; Peat, A. Rational design of potent non-nucleoside inhibitors of HIV-1 reverse transcriptase. *J. Med. Chem.* **2012**, *55*, 10601–10609.

(11) (a) La Regina, G.; Coluccia, A.; Brancale, A.; Piscitelli, F.; Gatti, V.; Maga, G.; Samuele, A.; Pannecouque, C.; Schols, D.; Balzarini, J.; Novellino, E.; Silvestri, R. Indolylarylsulfones as HIV-1 non-nucleoside reverse transcriptase inhibitors. New cyclic substituents at the indole-2-carboxamide. *J. Med. Chem*. **2011**, *54*, 1587–1598; (b) La Regina, G.; Coluccia, A.; Brancale, B.; Piscitelli, F.; Gatti, V.; Maga, G.; Samuele, A.; Gonzalez, E.; Clotet, B.; Schols, D.; Esté, J. A.; Novellino, E.; Silvestri, R. New nitrogen containing substituents at the indole-2-carboxamide yield high potent and broad spectrum indolylarylsulfone HIV-1 non-nucleoside reverse transcriptase inhibitors. *J. Med. Chem.* **2012**, *55*, 6634–6638.

(12) Famiglini, V.; La Regina, G.; Coluccia, A.; Pelliccia, S.; Brancale, A.; Maga, G.; Crespan, E.; Badia, R.; Clotet, B.; Esté, J. A.; Cirilli, R.; Novellino, E.; Silvestri, R. New indolylarylsulfones as highly potent and broad spectrum HIV-1 non-nucleoside reverse transcriptase inhibitors. *Eur. J. Med. Chem.* **2014**, *80*, 101–111.

(13) Atkinson, J. G.; Hamel, P.; Girard, Y. A new synthesis of 3-arylthioindoles. *Synthesis* **1988**, *6*, 480–481.

(14) Menendez-Arias, L.; Alvarez, M. Antiretroviral therapy and drug resistance in human immunodeficiency virus type 2 infection. *Antiviral Res.* **2014,** *102*, 70–86.

(15) Zhao, Z.; Wolkenberg, S. E.; Lu, M.; Munshi, V.; Moyer, G.; Feng, M.; Carella, A. V.; Ecto, L. T.; Gabryelski, L. J.; Lai, L. T.; Prasad, S. G.; Yan, Y.; McGaughey, G. B.; Miller, M. D.; Lindsley, C. W.; Hartman, C. D.; Vacca, J. P.; Williams, T. M. Novel indole-3-sulfonamides as potent HIV non-nucleoside reverse transcriptase inhibitors (NNRTIs). *Bioorg. Med. Chem. Lett.*, **2008**, *18*, 554–559.

(16) Hsiou, Y.; Ding, J.; Das, K.; Clark, A. D., Jr.; Boyer, P. L.; Lewi, P.; Janssen, P. A.; Kleim, J. P.; Rosner, M.; Hughes, S. H.; Arnold, E. The Lys103Asn mutation of HIV-1 RT: a novel mechanism of drug resistance. *J. Mol. Biol*. **2001**, *309*, 437–445.

(17) Geitmann, M.; Unge, T.; Danielson, H.U. Interaction kinetic characterization of HIV-1 reverse transcriptase non-nucleoside inhibitor resistance. *J. Med. Chem*. **2006**, *49*, 2375–2387.

(18) Wodak, S. J.; Janin, J. Analytical approximation to the accessible surface area of proteins. *Proc. Natl. Acad. Sci. U.S.A.* **1980**, *77*, 1736–1740.

(19) Al-Kazimi, H. R.; Tarbell, D. S.; Plant, D. Study of the Schonberg rearrangement of diaryl thioncarbonates to diaryl thiolcarbonates. *J. Am. Chem. Soc.* **1955**, *77*, 2479–82.

(20) Piligram, K.; Korte, F. Thermolysis of *O,O*-dialkyl-S-arylthiophosphates. *Tetrahedron* **1965**, *21*, 1999–2013.

(21) E. Gonzalez-Ortega, E. Ballana, R. Badia, B. Clotet, J. A. Estè, Compensatory mutations rescue the virus replicative capacity of VIRIP-resistant HIV-1. *Antiviral Res*. **2011**, *92*, 479–483.

(22) A. N. Van Nhien, C. Tomassi, C. Len, J. L. Marco-Contelles, J. Balzarini, C. Pannecouque, E. De Clercq, D. Postel, First synthesis and evaluation of the inhibitory effects of aza analogues of TSAO on HIV-1 replication. *J. Med. Chem*. **2005**, *48*, 4276–4284.

(23) G. Maga, M. Amacker, N. Ruel, U. Hubsher, S. Spadari, Resistance to nevirapine of HIV-1 reverse transcriptase mutants: loss of stabilizing interactions and thermodynamic or steric barriers are induced by different single amino acid substitutions. *J. Mol. Biol*. **1997**, *274*, 738–747.

(24) Férir, G.; Petrova, M.; Andrei, G.: Huskens, D.; Hoorelbeke, B.; Snoeck, R.; Vanderleyden, J.; Balzarini, J.; Bartoschek, S.; Brönstrup, M.; Süsmuth, R.; Schols. D. The lantibiotic peptide labyrinthopeptin A1 demonstrates broad anti-HIV and anti-HSV activity with potential for microbicidal applications. *PLoS One* **2013**, *8*, e64010.

(25) Ren, J.; Milton, J.; Weaver, K. L.; Short, S. A.; Stuart, D. I.; Stammers, D. K. Structural basis for the resilience of efavirenz (DMP-266) to drug resistance mutations in HIV-1 reverse transcriptase. *Struct. Fold. Des*. **2000**, *8*, 1089–1094.

(26) Ren, J.; Nichols, CE.; Chamberlain, PP.; Weaver, KL.; Short, SA.; Stammers, DK. Crystal structures of HIV-1 reverse transcriptases mutated at codons 100, 106 and 108 and mechanisms of resistance to non-nucleoside inhibitors. *J Mol Biol.* **2004**, *336*, 569–78.

(27) Ren, J.; Nichols, C.; Bird, L.; Chamberlain, P.; Weaver, K.; Short, S.; Stuart, D. I.; Stammers, D. K. Structural mechanisms of drug resistance for mutations at codons 181 and 188 in HIV-1 reverse transcriptase and the improved resilience of second generation nonnucleoside inhibitors. *J. Mol. Biol*. **2001**, *312*, 795–805.

(28) MOE version 2010, **2010**, C.C.G., 1010 Sherbrooke St. West, Suite 910, Montreal, Canada, H34 2R.

(29) Korb, O.; Stutzle, T.; Exner, T. E. PLANTS: Application of ant colony optimization to structure-based drug design. In ant colony optimization and swarm intelligence, Proceedings of the 5th International Workshop, ANTS; Dorigo, M.; Gambardella, L. M.; Birattari, M.;

Martinoli, A.; Poli, R. Stutzle, T.. Eds. Lecture Notes in Computer Science, Series 4150; Springer: Berlin, **2006**; pp 247–258.

(30) Desmond Molecular Dynamics System, version 2.4, D. E. Shaw Research, New York, NY, **2010**; Maestro-Desmond Interoperability Tools, version 2.4, Schrödinger, New York, NY, **2010**.

(31) Guo, Z.; Mohanty, U.; Noehre, J.; Sawyer, T. K.; Sherman, W.; Krilov, G. Probing the alpha-helical structural stability of stapled p53 peptides: molecular dynamics simulations and analysis. *Chem. Biol. Drug Des*. **2010**, *75*, 348–359.

(32) Jorgensen, W. L.; Maxwell, D. S.; TiradoRives, J. Development and testing of the OPLS all-atom force field on conformational energetics and properties of organic liquids. *J. Am. Chem. Soc*. **1996**, *118*, 11225–11236.

(33) Kaminski, G. A.; Friesner, R. A.; Tirado-Rives, J.; Jorgensen, W. L. Evaluation and reparametrization of the OPLS-AA force field for proteins via comparison with accurate quantum chemical calculations on peptides. *J. Phys. Chem. B* **2001**, *105*, 6474–6487.

(34) Wohnsland, F.; Faller, B. High-throughput permeability pH profile and high-throughput alkane/water log P with artificial membranes. *J. Med. Chem.* **2001**, *44*, 923-930.

(35) Sugano, K.; Hamada, H.; Machida, M.; Ushio, H. High throughput prediction of oral absorption: improvement of the composition of the lipid solution used in parallel artificial membrane permeation assay. *J. Biomol. Screen.* **2001**, *6*, 189-196.

TOC Graphic

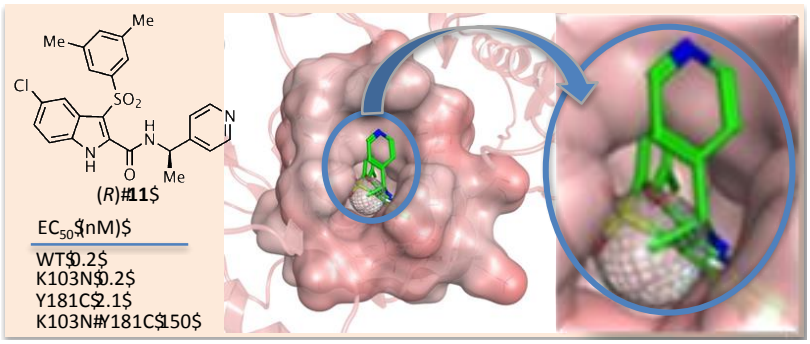
Me
Me
Cl
SO2
H
N
N
H
O
N
Me
(R)-11
EC50 (nM)
WT 0.2
K103N 0.2
Y181C 2.1
K103N+Y181C 150